SLAC-PUB-848
January 1971

RADIATIVE CORRECTIONS TO ELECTRON SCATTERINGS*

Yung-Su Tsai

Stanford Linear Accelerator Center
Stanford University, Stanford, California 94305, U.S.A.

ABSTRACT

Radiative corrections to the electron scattering from nucleons and nuclei at high energies (> 50 MeV) are considered. Many formulas in the Mo and Tsai's article in Review of Modern Physics are improved and better derivations of them are presented. The effects of the straggling of electrons in the medium due to both the external bremsstrahlung and the ionization are included in the radiative corrections. A method for dealing with the radiative corrections to the scattering from a target material with a large Z is proposed. We suggest that the proper way to deal with the radiative corrections to the coincidence experiments is in terms of the energy-momentum distribution and the density matrix of the virtual photon exchanged; formulas needed for dealing with the problem this way are presented.

(Lectures given at "Nato Advanced Institute on Electron Scattering and Nuclear Structure at Cagliari, Italy, September 1970.)

*Work supported by the U.S. Atomic Energy Commission.

1. INTRODUCTION

Professor Bosco asked me to give a course in radiative corrections to the electron scatterings from nuclei including those to the coincidence experiments. This note is an expanded version of the lectures I gave at the summer institute. The author benefited greatly from the discussions with many people at the institute. The note was expanded and altered considerably from the original one in order to answer many questions raised at the institute.

Why do we need radiative corrections? Let us consider an electron scattering from a nucleus. The Feynman diagram representing the process in the lowest order of α is given by Fig. 1. The theoretical analysis of the process is most convenient in terms of Fig. 1 (see Appendix A). However if one actually scatters an electron from a nucleus, the probability of the process described by Fig. 1 occurring is strictly speaking zero. Several corrections have to be applied to the experimental data before one can extract the idealized cross section represented by Fig. 1. In the first place it is impossible to scatter a charged particle without emitting an infinite number of soft photons (Bloch and Nordsieck[1]). Because of its small mass the photon emission by the electron is much more important than the photon emission by the hadron target system. This is especially true for experiments designed to investigate the nuclear structure where the target particle is usually heavier than the proton and the incident electron beam energy is usually less than one GeV. The photon emission by hadrons is negligible compared with that by electrons until the energies of these hadrons become relativistic.[2] We shall ignore the bremsstrahlung emission by the target system except when treating the elastic scattering. The order of magnitude of the effects of the bremsstrahlung emission by the target system can be inferred from the results of the calculation given for the elastic scattering.[2,3,4] The formulas for the radiative corrections are usually derived under the assumption of one photon exchange between the electron current and the hadron current.[5] For a target with a high atomic number Z, it is well known that one photon exchange is a bad approximation and the method of phase shift analysis using the exact Coulomb wave function (with form factors) must be used.[6] It is also known that a good approximation to the results of the phase shift analysis can be obtained by a distorted wave Born[7] approximation in which most of the energy and momentum transfer from the electron to the nuclear system is carried by a single photon and the rest of the Coulomb interaction consists of exchanges of infinite number of soft photons between the electron and the hadron.

It is well known that the probability of soft photon emission is proportional to the cross section for no photon emission (see Eqs. (2.3) and (2.4)) and the proportionality constant depends upon q^2, E_s (the incident electron energy) and E_p (the outgoing electron energy) only logarithmically. Since the distorted wave Born approximation shows that the effective E_s, E_p and q^2 in the problem are not appreciably changed by the Coulomb distortion, we expect this proportionality constant, which we shall refer to as radiative corrections, should not change appreciably. For a hard photon emission the situation is less clear. In Chapter 3, we propose a procedure to handle this problem based on the following observations:

1. The Coulomb distortion can in a certain sense be regarded as some change in form factors.
2. One can[2] always cook up a peaking approximation formula which reproduces the exact Born approximation calculation of the radiative tail corresponding to a particular set of form factors, even though it is difficult to find a universal peaking approximation formula which is good for all form factors.
3. Since the Born approximation does give gross features of the electron-nucleus scattering even for a large Z material, we expect the peaking

approximation formula which reproduces the Born approximation result well will also be good for the Coulomb distorted cross sections.

The Coulomb distortion does not represent the entire effects of multiple photon exchange. For example it does not take into account the possibility that in the two-photon exchanges, the hadron intermediate states can be an excited state instead of the ground state.[8] The estimate of this effect is highly model dependent. However some model calculations[9] show that the effect is significant only in the region of diffraction minima. Since all the calculations are numerically unreliable, all one has learned from this type of model calculation up to now is that when doing a phase shift analysis it is illusory to try to fit the region of diffraction minimum beyond the accuracy comparable to the magnitude of the dispersion effects. Similar to the fact that one-photon exchange formalism gives the gross features of the electron scattering, one real photon emission gives the gross features of the radiative corrections except in the infrared limit. Suppose a charged particle lost a certain amount of energy Δ by radiation. We know from Bloch-Nordsiek[1] theorem that Δ is shared by an infinite number of photons. However because of $1/k_i$ dependence for the probability of emitting the ith photon, it is much more probable for one of the photons to take up practically all the energy available and only a small fraction of Δ is shared by the rest of the photons than many photons sharing almost equally the available energy. This phenomenon is very similar to the fact that in Coulomb scattering it is most probable that most of the energy and momentum transfer is carried by a single virtual photon. All the corrections mentioned above are higher order α corrections to the process under consideration. In practice it is convenient (actually necessary) to consider at the same time the straggling of the electrons in passing through the medium before and after the scattering.[10,11,12] The bremsstrahlung emission of the electron in passing through the medium before and after the scattering is called the external bremsstrahlung whereas the bremsstrahlung emission during the collision is called the internal bremsstrahlung. The internal bremsstrahlung is proportional to the target thickness T, but the external bremsstrahlung is proportional to T^2. Another T^2 effect is the ionization, which is sometimes called the Landau straggling.[13] The internal and external bremsstrahlungs have almost identical dependence on the energy loss Δ, but the ionization loss behaves quite differently from the bremsstrahlung. The straggling of an electron in passing through a medium due to the combined effects of the external bremsstrahlung and the ionization is discussed in Appendix B. In Appendix C, we show that the effect of the straggling can be approximated by assuming that the scattering took place at exactly half the path length, the error is less than 1% if T is less than 0.1. We also show how the two-dimensional integration with respect to dE'_p and dE'_s can be approximated by two line integrations. The reader is advised to read the appendices before reading the text. In the text we deal mainly with how to put together various pieces of formulas, derived in the appendices and elsewhere, in order to actually carry out the radiative corrections to the experimental data.

There are some differences in the treatment of the radiative corrections to the multi-GeV ep scattering and the low energy (100 MeV) e-nucleus scattering. In the ep scattering there are only about three or four broad bumps (1238, 1525, 1700 and 1900 MeV ?) each with a width of around 100 MeV. These bumps are all above the pion threshold and hence lie on top of the continuum (see Fig. 2). In the electron nucleus scattering the levels are much more numerous, the intrinsic width of these levels are in general negligible, and many of these levels are below the threshold of the continuum. In the ep scatterings only the elastic peak needs a special treatment, and all the resonances can be treated the same way — as we treat the continuum. In the e nucleus scattering all experimentally resolvable levels are narrow and can be regarded as discrete, the apparent widths of these levels are mostly due to internal and external bremsstrahlung, Landau straggling, the energy width in the incident beam and the energy resolution in the detection system.

It should be emphasized that experiments should be planned from the beginning so that the radiative correction can be carried out reliably. For example in order to carry out the radiative corrections we need to have many spectra (each with a different incident energy) at each scattering angle. The greater the number of spectra the more reliable are the interpolations and extrapolations needed to carry out the radiative corrections.[2] Now in order to separate out the two form factors and determine their q^2 and ν dependence it is necessary to perform experiments at different scattering angles and different incident energies. The two kinematical regions covered by the two above requirements should have a maximum overlap.[2] The effect of the internal bremsstrahlung is roughly the same as that given by two external radiators with one placed before and one after the scattering, each of thickness[2]

$$t_r = b^{-1}(\alpha/\pi)\left[\ln(-q^2/m^2) - 1\right]$$

radiation lengths, where b is a number very close to 4/3.

Hence in order to reduce the effect due to the straggling, the target thickness should be chosen less then $2\,t_r$.

It is also important to place the target so that the path length of the target is constant for a fixed scattering angle independent of where the interaction takes place in order to simplify the calculation of the straggling effects. This can be accomplished easily by rotating the target of a uniform thickness such that the angle between the incident electron and the target surface is equal to the angle between the outgoing electron and the target surface.[11] We follow closely the notations of MT;[2] they are summarized below for easy reference. We use the convention h=c=1. The metric used is such that $p\cdot s = E_s E_p - \mathbf{p}\cdot\mathbf{s}$. Components of four vectors and angles are all in the laboratory system.

$S=(E_s, \mathbf{s})$: four momentum of the incident electron.

$p=(E_p, \mathbf{p})$: four momentum of the outgoing electron.

$t=(M, 0)$: four momentum of the target particle.

$k=(\omega, \mathbf{k})$: four momentum of the real photon emitted.

$p_f=s+t-p-k$: four momentum of the final hadronic system.

$u=(u_0, \mathbf{u}) = s+t-p=p_f+k$

$u^2=2m^2+M^2-2(s\cdot p)+2M(E_s-E_p)$ = missing mass squared.

$M_f^2=p_f^2$

$q^2=(s-p-k)^2=(p_f-t)^2$

θ=scattering angle

T=total path length in unit of radiation length x_0 of the electron in the target before and after the scattering.

Z=atomic number of the target nucleus.

A=atomic weight of the target nucleus.

$N=6.023\times10^{23}$=avogadro's number.

$r_0=2.818\times10^{-13}$ cm = classical radius of an electron.

$\sigma(E_s, E_p) \equiv \frac{d\sigma(E_s, E_p)}{d\Omega\, dE_p}$ = cross section with the incident electron energy E_s and the outgoing electron energy E_p after the radiative corrections. When Z is small this cross section is given by the lowest order Born approximation. When Z is large, this is the cross section to be analyzed by the distorted wave Born approximation.

$\sigma_r(E_s, E_p) \equiv \dfrac{d\sigma_r(E_s, E_p)}{d\Omega\, dE_p}$ = the measured cross section if the target has zero thickness so that no straggling occurs.

$\sigma_b(E_s, E_p) \equiv \dfrac{d\sigma_b(E_s, E_p)}{d\Omega dE_p}$ = a hypothetical cross section where $\sigma(E_s, E_p)$ was altered by the external bremsstrahlung only.

$\sigma_{exp}(E_s, E_p) \equiv \dfrac{d\sigma_{exp}(E_s, E_p)}{d\Omega dE_p}$ = the measured cross section containing effects due to virtual photon, internal and external bremsstrahlung and ionization.

$$\omega_s = \frac{1}{2}\,(u^2 - M_f^2)/\left[M + E_p(1-\cos\theta)\right] \quad (1.1)$$

= The maximum energy of a photon which can be emitted along the direction of the incident electron if the mass of the final hadron system is M_f.

$$\omega_p = \frac{1}{2}\,(u^2 - M_f^2)/\left[M + E_s(1-\cos\theta)\right] \quad (1.2)$$

= The maximum energy of a photon which can be emitted along the direction of the outgoing electron if the mass of the final hadron system is M_f.

$$q_s^2 = -2(E_s - \omega_s)\,E_p(1-\cos\theta) \quad (1.3)$$

$$q_p^2 = -2E_s(E_p + \omega_p)(1-\cos\theta) \quad (1.4)$$

$$v_s = \omega_s/E_s \quad (1.5)$$

$$v_p = \omega_p/\left(E_p + \omega_p\right) \quad (1.6)$$

We would like to introduce a very useful quantity called the effective non-radiative cross section:

$$\sigma_{eff}(E_s, E_p) = F(q'^2, T)\ \sigma(E_s-\Delta_s, E_1+\Delta_p) \tag{1.7}$$

We first introduce a few quantities which were used in the discussion of the straggling effect

$$a = \frac{2\pi N\alpha^2}{m}\ \frac{Z}{A}\ (\text{centimeter})^{-2} = 0.154\ \text{MeV}\ \frac{Z}{A}$$

= a parameter used in the ionization loss, see Eq. (B.1).

x_0 = unit radiation length in gm/cm^2.

$$\Delta_s = a\,\frac{T}{2}\,x_0\left[\ln \frac{3\times 10^9\ a\ \frac{T}{2}\ x_0\ E_s^2}{m^2 Z^2} - 0.5772\right] \tag{1.8}$$

= the most probable energy loss of the incident electron due to the ionization after passing through a target material of thickness T/2.

Δ_p = similar quantity as above except that E_s is replaced by E_p. (1.9)

$b \approx 4/3$ (see Eq. (B.5)).

As will be shown in Appendix C, when $T \ll 1$ the effect of the external bremsstrahlung can be approximated by assuming that the scattering took place at exactly half the path length. The error involved is less than 1% when $T < 0.1$. We shall make this approximation in order to avoid the integration with respect to the path of the electron. Under this approximation the effective incident energy is equal to $E_s-\Delta_s$ and the effective outgoing energy is equal to $E_p+\Delta_p$. This explains why we have $E_s-\Delta_s$ and $E_p+\Delta_p$ in Eq. (1.7). The momentum transfer squared for the nonradiative process corresponding these effective incident and outgoing energies is

$$q'^2 = -4(E_s-\Delta_s)(E_p+\Delta_p)\ \sin^2 \theta/2\ . \tag{1.10}$$

The factor $F(q'^2, T)$ in Eq. (1.7) is defined in Eq. (2.8). This factor is independent of the photon energy in the infrared limit. This factor occurs independently of whether photons are emitted by electrons or not, and hence it behaves as if it were a part of the hadron form factors. Therefore it is convenient to use σ_{eff} instead of σ in performing the radiative correction to the peak and in calculating the radiative tail. After all the experimental data are reduced into σ_{eff}, we may divide it by $F(q'^2, T)$ and obtain σ. The best way to handle Δ_s and Δ_p is to redefine the incident and outgoing electron energy from the beginning as $E_s - \Delta_s$ and $E_p + \Delta_p$ respectively. If this is done we can forget about Δ_s and Δ_p in all the subsequent calculations. We shall assume that this is done in order to save writing and computation time. In other words we shall adopt a convention that whenever Δ_s and Δ_p are absent from the formula, it is to be understood that E_s and E_p really mean $E_s - \Delta_s$ and $E_p + \Delta_p$ respectively.

Examples: $E'_p - E_p = \omega_p$ really means $E'_p - E_p - \Delta_p = \omega_p$.

$E_s - E'_s = \omega_s$ really means $E_s - \Delta_s - E'_s = \omega_s$.

$\sigma(E_s, E_p)$ really means $\sigma(E_s - \Delta_s, E_p + \Delta_p)$.

Let us give the order of magnitude of $\Delta_{s,p}$. The ionization loss Δ_0 for a particle of energy E_0 is quite insensitive to E_0, and is roughly proportional to the target thickness in gm/cm^2 as can be seen from Eqs. (1.8) and (1.9). For most materials other than hydrogen, Δ_0/x, where x is the thickness in gm/cm^2, is roughly 1 (for lead) to 2 (for deuterium) MeV per gm/cm^2. Hydrogen is an exceptional case because $Z/A=1$, whereas for most other materials $Z/A \sim 0.5$. For hydrogen Δ_0/x is 4 to 5 MeV per gm/cm^2 depending upon the energy.

2. RADIATIVE CORRECTION TO THE DISCRETE LEVELS

Let p_f be the four momentum of the final hadron system and k be the four momentum of the photons emitted, then obviously

$$u^2 \equiv (p_f+k)^2 \geq p_f^2 \equiv M_f^2 . \tag{2.1}$$

This relation tells us that the radiative tail from the lighter M_f can affect the measurement of heavier M_f but not vice versa. The elastic scattering has the smallest M_f, hence the radiative tail from the elastic peak affects all the higher M_f states in the experiment. Thus we first apply the radiative corrections to the elastic peak, then calculate the radiative tail from the elastic peak. The elastic radiative tail is then subtracted from the spectrum. Apply the same procedure to the first excited state and then to the second and so forth until we reach the threshold of the continuum state or until the energy levels become so closely spaced that it is impossible to resolve these levels experimentally. The continuum state can be regarded as a summation of many discrete levels hence the principle involved is the same as the discrete case but in practice it can be handled in a more efficient way (see Chart 4 and Appendix C).

In Fig. 3 an elastic peak and two other discrete peaks are shown. As mentioned previously, in nuclear physics (not in elementary particle physics), the intrinsic widths of the excited states are usually negligible compared with the width due to

a. Internal bremsstrahlung

b. External bremsstrahlung

c. Landau straggling

d. Finite energy spread in the incident beam and the finite momentum resolution in the detection system.

Suppose we are interested in the radiative corrections to the jth peak. Let us arbitrarily choose a point $E_{p\,min}$ between the jth peak and the j+1th peak and define

$$\frac{d\sigma_{j,exp}}{d\Omega}(\Delta E) \equiv \int_{E_{p\,min}}^{E_{p\,max}} \frac{d\sigma_{j,exp}}{d\Omega_p dE_p} E_p \tag{2.2}$$

where $\Delta E = E_p^{peak} - E_{p\,min}$. Notice that $E_{p\,max} \neq E_p^{peak}$. The expression for the radiative corrections is relatively simple if two neighboring levels are separated by a distance much greater than the width due to the Landau straggling and the experimental resolution. If this is so, ΔE in Fig. 3 can always be chosen much larger than the width but small enough so that the cross section at incident energies E_s and $E_s - R\Delta E$ are not appreciably different (less than 10%) and we can write the radiative corrections to the jth peak as (see Appendix C)

$$\frac{d\sigma_{j,exp}}{d\Omega}(\Delta E) = \frac{d\sigma_j^{eff}(E_s)}{d\Omega} \left(\frac{R\Delta E}{E_s}\right)^{T'} \left(\frac{\Delta E}{E_p^{peak}}\right)^{T'} \times \left(1 - \frac{\xi}{\Delta E}\right) \tag{2.3}$$

where

$$\frac{d\sigma_j^{eff}(E_s)}{d\Omega} \equiv F(q^2, T) \frac{d\sigma_j(E_s)}{d\Omega} . \tag{2.4}$$

$d\sigma_j/d\Omega$ is the nonradiative cross section we want to deduce from the data. $d\sigma_j^{eff}(E_s)/d\Omega$ is the effective nonradiative cross section needed in Chapter 3 to calculate the radiative tail. $R\Delta E$ is the maximum energy of photons which can be emitted along the incident electron direction. R is defined in Eq. (C.19). ξ is a parameter in Landau straggling and is given by

$$\xi = 0.154\, Z/A\; Tx_0 \text{ MeV} , \tag{2.5}$$

T = target thickness in units of radiation length,

x_0 = unit radiation length in gm/cm^2.

$$T' \equiv b\left(\frac{T}{2}+t_r\right), \quad t_r = b^{-1}\,\frac{\alpha}{\pi}\left(\ln \frac{2(s\cdot p)}{m^2} - 1\right) . \qquad (2.7)$$

$F(q^2,T)$ represents all other corrections which are independent of ΔE:

$$\begin{aligned} F(q^2,T) &= 1 + 0.5772\ bT \\ &+ \frac{2\alpha}{\pi}\left[\frac{-14}{9} + \frac{13}{12}\ln \frac{-q^2}{m^2}\right] \\ &- \frac{\alpha}{2\pi}\ln^2\left(\frac{E_s}{E_p}\right) \\ &+ \frac{\alpha}{\pi}\left[\frac{1}{6}\pi^2 - \Phi\left(\cos^2 \frac{\theta}{2}\right)\right] . \end{aligned} \qquad (2.8)$$

The term 0.5772 bT comes from the normalization factor

$$1/\Gamma(1+bT) \approx 1 + 0.5772\ bT \qquad (2.9)$$

in the external bremsstrahlung. (See Appendix B for further discussion on this factor.)

The factor

$$\frac{2\alpha}{\pi}\left[\frac{-14}{9} + \frac{13}{12}\ln \frac{-q^2}{m^2}\right]$$

is the sum of the vacuum polarization (e^+e^- bubble in the photon propagator) and the noninfrared part[3] of the vertex correction:

$$\delta_{vac} = \frac{2\alpha}{\pi}\left[(-5/9) + \frac{1}{3}\ln(-q^2/m^2)\right] \qquad (2.10)$$

and

$$\delta_{\text{vertex}} = \frac{2\alpha}{\pi}\left[-1+\frac{3}{4}\,\ln(-q^2/m^2)\right] \quad . \tag{2.11}$$

The term[2,3,4,5] $-(\alpha/2\pi)\,\ln^2(E_s/E_p)$ is an approximation to a sum of two Spence functions:

$$\Phi\left(\frac{E_p-E_s}{E_p}\right)+\Phi\left(\frac{E_s-E_p}{E_s}\right) \approx -\frac{1}{2}\,\ln^2\frac{E_s}{E_p} \quad . \tag{2.12}$$

This term can be regarded as a correction to the peaking approximation in the internal bremsstrahlung. This term will be the only correction necessary if the nonradiative cross section is assumed to be constant when integrating with respect to the energy and angle of the photon. The smallness of this term indicates that the peaking approximation is indeed good if the variation of the nonradiative cross section can be ignored.

The last term in Eq. (2.8) is the term in the Schwinger[15] corrections sometimes ignored. It was written in terms of the Spence function by Kallen.[14] This term is zero at $\theta=0$ and monotonically increases with θ. When $\theta=\pi$, the Spence function vanishes and this term has the maximum value of $\alpha\pi/6 = 0.0037$. Hence the correction due to this term is at most 0.37%.

The Spence function[16] is defined as

$$\Phi(x) = \int_0^x \frac{-\ln|1-y|}{y}\,dy \tag{2.13}$$

The following properties of $\Phi(x)$ are useful for its numerical evaluation:

$$\Phi(x) = x+\frac{1}{4}x^2+\frac{1}{9}x^3+\ldots+(x^n/n^2)+\ldots\,, \text{ if } |x| \leq 1\,;$$

$$\Phi(1) = \frac{1}{6}\pi^2 \quad\text{and}\quad \Phi(-1) = -\frac{1}{12}\pi^2\,;$$

for $x > 1$,

$$\Phi(x) = -\frac{1}{2}\ln^2|x| + \frac{1}{3}\pi^2 - \Phi(1/x) ;$$

and for $x < -1$

$$\Phi(x) = -\frac{1}{2}\ln^2|x| - \frac{1}{6}\pi^2 - \Phi(1/x) .$$

From the above we can show easily

$$0 \leq \Phi(1) - \Phi(x) \leq \Phi(1)\,(1-x) \quad , \quad \text{when } 0 < x < 1 .$$

Hence the last term in Eq. (2.8) satisfies the inequality,

$$0 \leq \frac{\alpha}{\pi}\left[\frac{1}{6}\pi^2 - \Phi(\cos^2\theta/2)\right] \leq \frac{\alpha\pi}{6}\sin^2\frac{\theta}{2} . \tag{2.14}$$

The equality in the second $\leq$ is satisfied when $\theta=0$ and π. This term was originally derived by Schwinger[15] for the nonrecoil case. If $E_s \gg E_p$ in the laboratory system, one would not obtain this simple expression. This term comes from the noninfrared divergent part of the soft photon emission cross section. The general expression corresponding to this term for an arbitrary recoil and energy loss can be written as (see YFS[17])

$$\frac{\alpha}{\pi}(s\cdot p)\int_{-1}^{1} G_{s,p}(x)\,\frac{dx}{p_x^2} \tag{2.15}$$

where s and p are four momenta of the incident and outgoing electrons respectively.

$$2p_x = (1+x)s + (1-x)p ,$$

$$p_x^2 = \frac{1}{2}\left[(1+x^2)\,m^2 + (1-x^2)\,(s\cdot p)\right]$$

and

$$G_{s,p}(x) = \frac{E_x - |\underset{\sim}{p}_x|}{2|\underset{\sim}{p}_x|}\ln\left(\frac{E_x + |\underset{\sim}{p}_x|}{E_x - |\underset{\sim}{p}_x|}\right) + \ln\frac{(E_x + |\underset{\sim}{p}_x|)}{2E_x} .$$

If we ignore the mass of the electron and the recoil, we have

$$E_x = E_s = E_p \quad \text{and} \quad |\underline{p_x}| = E_x \left(1 - (1-x^2)\sin^2\frac{\theta}{2}\right)^{1/2} \equiv E_x \xi \ ,$$

and Eq. (2.20) can then be reduced into

$$\frac{2\alpha}{\pi} \sin\frac{\theta}{2} \int_{\cos\frac{\theta}{2}}^{1} \left[\frac{1}{1-\xi} \ln\frac{1+\xi}{2} - \frac{1}{1+\xi} \ln\frac{1-\xi}{2}\right] \frac{d\xi}{\left(\xi^2 - \cos^2\frac{\theta}{2}\right)^{1/2}}$$

which is precisely Eqs. (2.97) and (2.105) of Schwinger.[15]

We have ignored the bremsstrahlung emission from the hadron system in Eq. (2.3) because we would like to use this equation for all the discrete levels. The effect of the bremsstrahlung emission by hadrons in the elastic scattering can be seen from the numerical examples given in Tables I and II of Mo and Tsai.[2] If you think the effect is important, then the following formula must be used instead of Eq. (2.3):

$$\frac{d\sigma_{exp}}{d\Omega}(\Delta E) = G(q^2, T) \frac{d\sigma}{d\Omega} e^{\delta} \left(\frac{\Delta E R}{E_s}\right)^{bT/2} \left(\frac{\Delta E}{E_p^{peak}}\right)^{bT/2} \times \left(1 - \frac{\xi}{\Delta E}\right) \quad (2.16)$$

where δ is given by Eq. (II.6) of Mo and Tsai and

$$G(q^2, T) = 1 + 0.5772\, bT + \frac{\alpha}{\pi}\left[\frac{1}{6}\pi^2 - \Phi\left(\cos^2\frac{\theta}{2}\right)\right]. \quad (2.17)$$

3. RADIATIVE TAIL FROM A DISCRETE LEVEL

In this chapter we calculate the radiative tail from the peak $d\sigma_j^{eff}/d\Omega$ obtained in the previous chapter, so that its contribution to the spectrum can be subtracted. As shown in Appendix A we can calculate the radiative tail exactly in terms of two form factors describing $d\sigma_j/d\Omega$ if we assume (a) only one photon is exchanged between the electron current and the hadron current and (b) only one photon is emitted by the electron. However when Z is large, neither $d\sigma_j/d\Omega$ obtained in the previous chapter nor the bremsstrahlung process is given adequately by one photon exchange. Also in reality an infinite number of photons are emitted instead of just one photon. The rigorous derivation of radiative tails containing the effects due to multiple photon exchange and multiple photon emission does not exist. In general the radiative tail from the elastic peak is much more important than the radiative tails from the inelastic events. The reasons are twofold:

1. The elastic cross sections at a fixed angle is much larger than the inelastic cross sections in most of the experiments.
2. At a fixed angle the elastic cross section increases much more rapidly than the inelastic cross sections when the incident electron energy is reduced by the emission of photons.

In other words the tail from the elastic peak is large and long and its effect is felt all the way to the end of the spectrum but the tails from the inelastic events are small and short and its effect is felt only by their neighbors. From the numerical examples given in MT all versions of peaking approximations give excellent results when the energy loss due to radiation is smaller than 10% of the electron energy. Hence the peaking approximation can be safely used when calculating the tail from the inelastic events. In the peaking approximation the radiative tail is proportional to the nonradiative cross section, therefore we expect the effect due to the Coulomb distortion is automatically taken care of if we use the nonradiative cross section obtained in the previous chapter. For the tail from the elastic peak, there is again no problem when the energy loss is small (10%). When the atomic number Z is small so that one-photon exchange is a good approximation, we can calculate the probability of one-photon emission according to the formula given in Appendix A. The effects of the multiple photon emission is then obtained by multiplying the factors (see Appendix B)

$$\left(\frac{\omega_s}{E_s}\right)^{b\left(\frac{T}{2}+t_r\right)} \left(\frac{\omega_p}{E_p+\omega_p}\right)^{b\left(\frac{T}{2}+t_r\right)} = (v_s v_p)^{b\left(\frac{T}{2}+t_r\right)} \quad .$$

In Appendix C, Eq. (C.13), we have shown how to calculate the radiative tail assuming only the external bremsstrahlung. Using the results of Appendix B, Eq. (B.39), we can generalize Eq. (C.13) to include the effects due to the ionization, the internal bremsstrahlung and the virtual photon and obtain the radiative tail from the jth discrete level:

$$\frac{d\sigma_{j,\exp}(E_s)}{d\Omega\, dE_p} = (v_s v_p)^{b\left(\frac{T}{2}+t_r\right)} \Bigg[\frac{d\sigma^{\mathrm{eff}}_{j,r}(E_s, E_p)}{d\Omega dE_p}$$

$$+ \frac{M+(E_s-\omega_s)(1-\cos\theta)}{M-E_p(1-\cos\theta)} \frac{d\sigma^{\mathrm{eff}}_j(E_s-\omega_s)}{d\Omega} \left\{ \frac{bT}{2}\frac{1}{\omega_s}\phi(v_s) + \frac{\xi}{2\omega_s^2} \right\}$$

$$+ \frac{d\sigma^{\mathrm{eff}}_j(E_s)}{d\Omega} \left\{ \frac{bT}{2}\frac{1}{\omega_p}\phi(v_p) + \frac{\xi}{2\omega_p^2} \right\} \Bigg] \qquad (3.1)$$

where $\phi(v)$ is the shape of the bremsstrahlung multiplied by v and normalized such that $\phi(0)=1$. For example when the complete screening is applicable it can be written as Eq. (B.6). ξ is defined in Eq. (2.5). ω_s, ω_p, v_s and v_p were defined in Eqs. (1.1), (1.2), (1.5) and (1.6). t_r was defined in Eq. (2.7).

$d\sigma_j^{eff}/d\Omega$ is the cross section obtained in Eq. (2.4). Now we see why it is convenient to use σ^{eff} instead of σ in all of our intermediate steps. Had we not used σ^{eff}, our Eq. (3.1) would have looked much uglier and we would have wasted much computer time to compute $F(q_s^2, T)$, $F(q_p^2, T)$ Δ_s and Δ_p mentioned in the introduction.

$d\sigma_{j,r}^{eff}/d\Omega$ is the radiative tail due to one-photon emission in the absence of straggling. This cross section can be calculated in the following way:

1. When j represents an inelastic excitation (i.e., $M_j \neq M$), we may use the equivalent radiator method, because the radiative tail from an inelastic level is in general small and short, and the method gives an excellent result. This method is equivalent to dropping $d\sigma_{j,r}^{eff}/d\Omega$ from Eq. (3.1) and replacing T/2 by $T/2 + t_r$ inside the square bracket in Eq. (3.1).
2. When j represents the elastic scattering (i.e., $M_j = M$), we first apply the equivalent radiator method to obtain the order of magnitude of the tail. In the region where v_s and v_p are less than 0.1, the equivalent radiator method (ERM) gives a good result even for the elastic scattering. However when v_s is larger than 0.1, this method can give as much as 30% error according to the numerical examples given by MT^2. If the elastic radiative tail contributes less than 10% of the cross section, we might as well use ERM because the resultant error is at most 3% of the cross section.

3. If $Z\alpha \ll 1$, we may use the Born approximation, Eq. (A.24), to calculate $d\sigma^{eff}_{j,r}/d\Omega$. $W^j_1(q^2)$ and $W^j_2(q^2)$ in Eq. (A.24) have to be multiplied by $F(q^2, T)$ in order to calculate the effective cross sections.

4. For heavy nuclei we have to include the Coulomb distortion in order to obtain something similar to Eq. (A.24). Since this has never been done, we propose a temporary solution. The remarks made in 1 and 2 are applicable in heavy nuclei also. If ERM indicates a substantial radiative tail, a more reliable calculation is required.

We notice that in the method of equivalent radiators we have assumed that the shape of the spectrum for the internal bremsstrahlung is equal to that of the external bremsstrahlung $\phi(v)$. This is of course totally ad hoc except when v is small compared with one. We can choose a better shape function using the Born approximation as a guide in the following way (see Chapter 1).

(i) Obtain an approximate expression for W_1F and W_2F using Eqs. (2.3) and (A.17) for the elastic peak. Strictly speaking this cannot be done when $z\alpha$ is large. Since for our present purpose only an approximately correct behavior of W_1 and W_2 is required, this can always be done.

(ii) Insert $FW_1(q^2)$ and $FW_2(q^2)$ obtained above into Eq. (A.24) and obtain the tail of the elastic peak in the Born approximation.

(iii) Write the elastic radiative tail in the form

$$\frac{d\sigma^{eff}_{0,r}}{d\Omega dE_p} = bt_r \left[\frac{M+(E_s-\omega_s)(1-\cos\theta)}{M-E_p(1-\cos\theta)} \frac{d\sigma^{eff}_0(E_s-\omega_s)}{d\Omega} \frac{1}{\omega_s} f(v_s) + \frac{d\sigma^{eff}_0(E_s)}{d\Omega} \frac{1}{\omega_p} f(v_p) \right] \tag{3.2}$$

f(v) is the function we want to determine. For example, it can be parameterized by

$$f(v) = 1 + c_1 v + c_2 v^2 .$$

Determine numerically c_1 and c_2 by comparing the tail obtained from Eq. (3.2) and that obtained in step (ii). FW_1 and FW_2 obtained in step (i) must be used to calculate $d\sigma_0^{eff}/d\Omega$ in Eq. (3.2) when making this comparison.

(iv) We claim that the correct radiative tail is obtained by using the original $d\sigma_0^{eff}/d\Omega$ in Eq. (3.2).

There is some uncertainty in the validity of the factor $(v_s v_p)^{b(T/2+t_r)}$ in Eq. (3.1)). We know that this factor is correct when v_s and v_p are small. R. Early's[19] numerical work suggests that this factor is correct even for large v_s and v_p for the external bremsstrahlung. Whether this is true or not for the internal bremsstrahlung is an open question. Yennie[18] suggested that this can be tested by calculating the cross section for emitting two real photons using perturbation theory. However in nuclear physics the value of $2\,s\cdot p=2E_sE_p(1-\cos\theta)$ is usually less than 1 GeV^2, hence bt_r is less than 0.033. Ignoring the recoil we have $v_s=v_p=v$, hence for the internal bremsstrahlung alone this factor can be written as $v^{2bt_r}=\psi$.

When $v=0.5$ and $bt_r=0.033$, we have $\psi=1-0.045$.

When $v=0.9$ and $bt_r=0.033$, we have $\psi=1-0.0066$.

These numerical examples show that the correction is minor, and it is unlikely that this factor contains a gross error.

4. RADIATIVE CORRECTIONS TO CONTINUOUS SPECTRA

After all the radiative tails from the discrete states have been subtracted from the spectrum we can proceed to do radiative corrections to the continuum. For the continuum it is safe to apply the equivalent radiator method. Since a continuum can be regarded as a sum of many discrete states we obtain the result by integrating Eq. (3.1) with respect to M_f^2. This was done in Appendix C (Eq. (C.23)). The result is

$$\frac{d\sigma_{exp}}{d\Omega dE_p} = \left(\frac{R\Delta}{E_s}\right)^{T'} \left(\frac{\Delta}{E_p}\right)^{T'} \left(1 - \frac{\xi}{(1-2T')\Delta}\right) \sigma^{eff}(E_s, E_p)$$

$$+ \int_{E_{s\,min}(E_p)}^{E_s - R\Delta} \sigma^{eff}(E_s', E_p) \left(\frac{E_s - E_s'}{E_p R}\right)^{T'} \left(\frac{E_s - E_s'}{E_s}\right)^{T'}$$

$$\times \left[\frac{T'}{E_s - E_s'} \, \phi\left(\frac{E_s - E_s'}{E_s}\right) + \frac{\xi}{2(E_s - E_s')^2}\right] dE_s'$$

$$+ \int_{E_p + \Delta}^{E_{p\,max}} \sigma^{eff}(E_s, E_p') \left(\frac{E_p' - E_p}{E_p'}\right)^{T'} \left(\frac{(E_p' - E_p)R}{E_s}\right)^{T'}$$

$$\times \left[\frac{T'}{E_p' - E_p} \, \phi\left(\frac{E_p' - E_p}{E_p'}\right) + \frac{\xi}{2(E_p' - E_p)^2}\right] dE_p' \,, \qquad (4.1)$$

where T' is given by Eq. (2.7). Δ should be chosen small enough so that $\sigma(E_s - R\Delta, E_p)$ and $\sigma(E_s, E_p + \Delta)$ are not appreciably (< 10%) different from $\sigma(E_s, E_p)$, but should be large enough so that ξ/Δ is less 0.1. The bremsstrahlung part is a convergent integration, hence the expression is correct even when Δ=0. The ionization part is a nonconvergent integration because we have used an asymptotic form. (See Eq. (B.34).)

However our result is quite independent of the choice of Δ. This can be verified by differentiating Eq. (4.1) with respect to Δ; we see that the result is equal to zero.

Our objective is to obtain $\sigma^{eff}(E_s, E_p)$ from the experimental cross section σ_{exp}. Since the desired cross sections $\sigma^{eff}(E_s', E_p)$ and $\sigma^{eff}(E_s, E_p')$ are also contained in the integrations, a procedure for unfolding is necessary. There are two ways of doing this. One is when the gross features of $\sigma(E_s, E_p)$ are known one can parameterize it and insert it into Eq. (4.1), adjusting the parameters until a satisfactory fit to the experimental data is obtained. Another method is to write Eq. (4.1) in the following form

$$\sigma^{eff}(E_s, E_p) = \left(\frac{R\Delta}{E_s}\right)^{-T'} \left(\frac{\Delta}{E_p}\right)^{-T'} \left(1 - \frac{\xi}{(1-2T')\Delta}\right)^{-1}$$

$$\left[\frac{d\sigma_{exp}(E_s, E_p)}{d\Omega\, dE_p} - \int_{E_{s\,min}(E_p)}^{E_s - R\Delta} (\ldots) - \int_{E_p+\Delta}^{E_{p\,max}(E_s)} (\ldots)\right] \qquad (4.2)$$

where the two integrations have the same expressions as those in Eq. (4.1). This equation implies that if $\sigma^{eff}(E_s', E_p')$ is known for $E_s' < E_s - R\Delta$ at constant E_p and $E_p' > (E_p+\Delta)$ at constant E_s, then $\sigma(E_s, E_p)$ can be obtained from the measured cross section $\sigma_{exp}(E_s, E_p)$. The cross section $\sigma\left[E_s' < E_{s\,min}(E_p), E_p\right]$ and $\sigma\left[E_s, E_p' > E_{p\,max}(E_s)\right]$ are equal to zero if the radiative tails from all the discrete levels have been subtracted from the measured cross section. Hence one can obtain the nonradiative cross section in the neighborhood of the threshold for the continuum along the line ab in Fig. 4. Knowing the cross sections on this strip we can calculate the cross section for the next strip and so forth until we unfold the cross sections within the entire area abc in Fig. 4.

Due to limitations on available accelerator time, usually the cross section is measured at many values of the outgoing electron energy E_p but only at a few values of the incident electron energy E_s. Hence the integration with respect to dE'_p can be carried out over the spectrum already unfolded. However some interpolations and extrapolations of the cross sections are required in performing the integration with respect to dE'_s. Since the cross section for a fixed value of the missing mass M_f varies only monotonically as a function of incident energy at a fixed angle, the interpolations and extrapolations should be carried out along the equimissing mass line rather than directly along the constant E_p line. There is no essential difficulty involved in the procedure just described. The only thing one needs is an efficient computer program to handle the entire unfolding automatically. For more details about unfolding and numerical examples, the reader should refer to MT. (Note that our Eqs. (4.1) and (4.2) are improved versions of the corresponding equations in MT.)

It should be emphasized that the first method mentioned is much simpler than the second. Another advantage of the first method is that after one is through with the analysis, $\sigma(E_s, E_p)$ is already in a nice parameterized form. Let us call the first method "the folding method" and the second method "the unfolding method".

5. RADIATIVE CORRECTIONS TO COINCIDENCE EXPERIMENTS

Suppose there are n hadrons in the final state in the inelastic electron scatterings

$$s+t \rightarrow p+p_1+p_2+ \dots + p_n\text{+photons}$$

s and p are four momenta of incident and outgoing electrons respectively. t is the four momentum of the target particle. $p_1, p_2 \dots p_n$ represent four momenta of n final hadrons. As mentioned previously, even though the actual number of photons emitted is infinite, most of the radiation loss is taken up by one photon, hence <u>for the kinematical consideration</u> one may approximate the infinite number of photons by one photon:

$$k_1+k_2+ \dots + k_\infty \rightarrow k$$

The phase space for the final state is

$$\frac{1}{(2\pi)^{3(n+2)}} \int \frac{d^3p}{2E_p} \int \frac{d^3k}{2\omega} \frac{d^3p_1}{2E_1} \frac{d^3p_2}{2E_2} \dots \frac{d^3p_n}{2E_n} \delta^4(p+p_1+p_2 \dots p_n+k-s-t) \quad (5.1)$$

We have assumed that the masses of all particles are known, hence each particle has only three degrees of freedom. We may use the δ function to eliminate the d^3p_n integration resulting in one dimentional δ function $\delta(p_n^2-M_n^2)$. Hence if we detect the particles $p, p_1, p_2, \dots, p_{n-1}$, the cross section would be a δ function, if no photons are emitted. If photons are emitted, this δ function enables us to determine the phase space of the photon from the momentum bites of $p, p_1, p_2, \dots, p_{n-1}$ detectors. When n=1, the experiment corresponds to a single arm spectrometer case for the excitation of a discrete level. The case for n=2 has been worked out by C. DeCalan and G. Fuchs.[20] Their results are given in terms of ΔE_p, ΔE_1 and M_2. As n becomes larger than 2, the radiative corrections become an unwieldy function of ΔE_p, ΔE_1, $\Delta E_2, \dots$ and $M_1 M_2 \dots$. Not only are these corrections difficult to calculate, they may be useless in practical applications for the following reasons:

1. When there are so many ΔE's, the phase space becomes so small that there may be too few events available for doing any analysis.
2. When there are many particles in the final state, very often some particles are neutral and escape detection.
3. The masses of the particles are often not known.

Apparently this approach to the problem is not very fruitful.

The work of DeCalan and Fuchs[20] can be generalized to

$$s+t \rightarrow p+p_1 + \text{all undetected hadrons} .$$

The technique must be similar to the way we generalized the radiative corrections to a discrete peak into the ones for

$$s+t \rightarrow p + \text{all undetected hadrons} .$$

Similar to the latter case the unfolding procedures will be involved. The details have not been worked out. However even if the details are worked out, it is doubtful that they can be used in practice.

I would like to suggest an alternative way to look at the problems of radiative corrections when the hadrons are detected in addition to the scattered electrons. If we ignore the interference between the bremsstrahlung emissions from electrons and hadrons and ignore the multiple photon exchange between them, the behavior of the hadron final states is completely determined by the density matrix and four-momentum distribution of the virtual photon. In the absence of the radiative corrections the four momentum of the virtual photon is q=s-p and the density matrix of the virtual photon is determined by the tensor:

$$t_{\mu\nu} = \frac{\mathrm{Tr}}{4} (\not{s}+m) \gamma_\mu (\not{p}+m) \gamma_\nu = s_\mu p_\nu + s_\nu p_\mu + \frac{q^2}{2} g_{\mu\nu} \tag{5.2}$$

When the radiative corrections and the straggling effects are included, both the four momentum of the virtual photon and the density matrix are given by certain distributions. Let us use the equivalent radiators to approximate the effects of the internal bremsstrahlung. The effects of the radiative corrections and straggling can then be simulated by placing one radiator of thickness $\frac{T}{2}+t_r$ before the scattering and another with the same thickness after the scattering. As mentioned previously it is convenient to treat the factor $F(2s\cdot p, T)$, which contains the vacuum polarization and vertex corrections etc., as if it were part of the hadron form factors when doing radiative corrections and only at the very end this factor is divided out from the result. We also use the convention that E_s represents the incident electron energy minus Δ_s and E_p means the actual outgoing electron energy plus Δp. Figure 5 gives a pictorial representation of our approximation. Because of the initial radiator $\left(\frac{T}{2}+t_r\right)$, the energy distribution of the electron just before the scattering is given by (see Appendix B)

$$I\left(E_s, E_s', \frac{T}{2}+t_r\right)dE_s' = \left(\frac{E_s-E_s'}{E_s}\right)^{b\left(\frac{T}{2}+t_r\right)} \frac{b\left(\frac{T}{2}+t_r\right)}{E_s-E_s'} \phi\left(\frac{E_s-E_s'}{E_s}\right) dE_s' \qquad (5.3)$$

where $\phi(v)$ represents the shape of the bremsstrahlung. We have ignored the straggling due to the ionization for simplicity. Similarly if the outgoing electron has energy E_p, then the energy distribution of the electron just after the scattering must be given by

$$I\left(E_p', E_p, \frac{T}{2}+t_r\right) dE_p' \qquad (5.4)$$

Knowing the energy distribution of the incident (E_s') and outgoing (E_p') electron energies, we can calculate the four-momentum distribution and the density matrix of the virtual photons immediately. Let us normalize the four-momentum distribution of the virtual photons by

$$\delta^4(q'-q)\, d^4q' \qquad (5.6)$$

when the radiative corrections are absent. The corresponding distribution when both the radiative corrections and the straggling are included can be calculated from

$$D(q') \, d^4q' = I\left(E_s, E_s', \frac{T}{2}+t_r\right) I\left(E_p', E_p, \frac{T}{2}+t_r\right) dE_s' \, dE_p' \tag{5.7}$$

where

$$q_0' = E_s' - E_p' \tag{5.8}$$

and

$$\underset{\sim}{Q}' = E_s' \underset{\sim}{e}_s - E_p' \underset{\sim}{e}_p \quad . \tag{5.9}$$

Since

$$q_0 = E_s - E_p \tag{5.10}$$

and

$$\underset{\sim}{Q} = E_s \underset{\sim}{e}_s - E_p \underset{\sim}{e}_p \quad , \tag{5.11}$$

we may write

$$q_0 - q_0' = (E_s - E_s') + (E_p' - E_p) \equiv \omega_s + \omega_p \tag{5.12}$$

and

$$\underset{\sim}{Q} - \underset{\sim}{Q}' = (E_s - E_s') \, \underset{\sim}{e}_s + (E_p' - E_p) \, \underset{\sim}{e}_p \equiv \omega_s \underset{\sim}{e}_s + \omega_p \underset{\sim}{e}_p \quad . \tag{5.13}$$

Equation (5.7) shows that only two variables in d^4q' are independent. Since the vector $\underset{\sim}{Q}'$ must be in the scattering plane, if we choose the direction of $\underset{\sim}{Q}$ to be the z axis and let $\underset{\sim}{s}$ and $\underset{\sim}{p}$ be on the xz plane then $\underset{\sim}{Q}'$ must be also on the xz plane (Fig. 6). From Eq. (5.13), the magnitude of $\underset{\sim}{Q}'$ is given by

$$Q' = \left[Q^2 - 2Q(\omega_s \cos\theta_{qs} + \omega_p \cos\theta_{qp}) + \omega_s^2 + \omega_p^2 + 2\omega_s\omega_p \cos\theta\right]^{1/2} \tag{5.14}$$

and the angle between $\underset{\sim}{Q}$ and $\underset{\sim}{Q}'$ is given by

$$\sin\theta_{qq'} = \frac{1}{Q'} (\omega_s \sin\theta_{qs} + \omega_p \sin\theta_{qp}) \quad . \tag{5.15}$$

q_0' is given by

$$q_0' = q_0 - \omega_s - \omega_p \quad . \tag{5.16}$$

Hence we may regard $q_0 - q_0' \equiv \Delta$ and $Q' \sin \theta_{qq'} \equiv q_x'$ as the independent variables, and obtain

$$dE_s' \, dE_p' = d\omega_s \, d\omega_p = \frac{1}{\sin \theta_{qp} - \sin \theta_{qs}} \, d\Delta \, dq_x' \quad , \tag{5.17}$$

$$\omega_s = \frac{\Delta \sin \theta_{qp} - q_x'}{\sin \theta_{qp} - \sin \theta_{qs}} \quad , \tag{5.18}$$

and

$$\omega_p = \frac{q_x' - \sin \theta_{qs}}{\sin \theta_{qp} - \sin \theta_{qs}} \quad . \tag{5.19}$$

From the elementary trigonometry, we obtain

$$\sin \theta_{qp} = E_s Q^{-1} \sin \theta \quad ,$$

and

$$\sin \theta_{qs} = E_p Q^{-1} \sin \theta \quad .$$

Hence the four momentum distribution of the virtual photon is

$$D(\Delta, q_x') \, d\Delta \, dq_x' = I\left(E_s, E_s + \omega_s, \frac{T}{2} + t_r\right) I\left(E_p - \omega_p, E_p, \frac{T}{2} + t_r\right) \frac{Q d\Delta \, dq_x'}{(E_s - E_p) \sin \theta} \tag{5.20}$$

where ω_s and ω_p are given by Eqs. (5.18) and (5.19) respectively.

Since I's are very peaked at $\omega_s = 0$ and $\omega_p = 0$, we see that $D(\Delta, q_x')$ must be very peaked at $q_x' = \Delta \sin \theta_{qp}$ and $q_x' = \Delta \sin \theta_{qs}$. From Eqs. (5.18) and (5.19) and $\omega_s \geq 0$, $\omega_p \geq 0$, we see that q_x' must satisfy

$$\Delta \sin \theta_{qs} \leq q_x' \leq \Delta \sin \theta_{qp} \tag{5.21}$$

or

$$E_p \Delta, \sin \theta / Q \leq q_x' \leq E_s \Delta \sin \theta / Q \quad . \tag{5.22}$$

The density matrix $t_{\mu\nu}$ is changed from Eq. (5.2) into a distribution

$$t'_{\mu\nu}\, dq'_x\, d\Delta = \frac{Tr}{4}\,(\not{s}'+m)\;\gamma_\mu(\not{p}'+m)\,\gamma_\nu\;\; I\left(E_s, E_s+\omega_s, \frac{T}{2}+t_r\right)$$

$$I\left(E_p-\omega_p, E_p, \frac{T}{2}+t_r\right)\; \frac{Q\,d\Delta\, dq'_x}{(E_s-E_p)\,\sin\theta}$$

In order to understand the behavior of $D(\Delta, q'_x)$ better, let us integrate

$$\int_0^{\Delta_{max}} d\Delta \int_{q'_{x\,min}}^{q'_{x\,max}} dq'_x\; D(\Delta, q'_x)$$

$$= \int_0^{\Delta_{max}} d\omega_s \int_0^{\Delta_{max}-\omega_s} d\omega_p\; b^2\left(\frac{T}{2}+t_r\right)^2 \frac{1}{\omega_s}\,\frac{1}{\omega_p}\left(\frac{\omega_s\,\omega_p}{E_s\,E_p}\right)^{b\left(\frac{T}{2}+t_r\right)}$$

$$= \left(\frac{\Delta_{max}}{E_s}\,\frac{\Delta_{max}}{E_p}\right)^{b\left(\frac{T}{2}+t_r\right)} \approx 1 - b\left(\frac{T}{2}+t_r\right)\left(\ln\frac{E_s}{\Delta_{max}} + \ln\frac{E_p}{\Delta_{max}}\right)$$

where $q'_{x\,max}$ and $q'_{x\,min}$ are given by Eq. (5.22). Suppose $b\left(\frac{T}{2}+t_r\right) = 0.025$, then in order to have 80% of the probability we must have

$$\ln\frac{E_s}{\Delta_{max}} + \ln\frac{E_p}{\Delta_{max}} = 8$$

or

$$\frac{(E_s E_p)^{1/2}}{\Delta_{max}} = 55\;.$$

This example shows the extent of energy spread of the virtual photon beam. The angular spread can be evaluated from Eq. (5.22).

The average angular spread for a fixed Δ is

$$\bar{\theta}_{qq'} \approx \frac{\overline{q'_x}}{Q} = \frac{(q'_{x\,max}\, q'_{x\,min})^{1/2}}{Q} = \frac{(E_s E_p)^{1/2}}{Q^2} \Delta \sin\theta \ .$$

If we use the value of Δ obtained above, we have

$$\bar{\theta}_{qq'} = \frac{E_s E_p}{Q^2} \frac{\sin\theta}{55} \ .$$

The important thing to remember is that the angular spread of the virtual photon is in the scattering plane only. Hence if we measure the hadron production angle in the plane perpendicular to the plane of the electron scattering, the error to this angular spread is minimized.

In conclusion, the energy and angular spreads of the virtual photon beam due to the radiative corrections and stragglings are not worse than the experiment using the semimonochromatic photon beam[20a] from $e^+e^- \rightarrow 2\gamma$. If the photon beam from the latter can be used in performing the experiments, there is no reason why the virtual photon beam with known energy and angular spread cannot be successfully used.

Our expression can be simplified further if we assume that only one photon is emitted. In this case q'_x can take only two values: $q'_{x\,max}$ when $\Delta=\omega_p$, and $q'_{x\,min}$ when $\Delta=\omega_s$. Hence under this approximation the distribution of the virtual photon is a function of only one variable Δ or q'_x. This approximation is not bad because, as we stated in the introduction, it is most probable that most of the energy loss Δ is taken up by one photon even though infinitely many soft photons are always emitted at the same time.

In order to make our presentation as simple as possible, we have used the angular peaking approximation for the internal bremsstrahlung and also ignored the Landau straggling. The latter effect can be restored into our consideration easily. The effect due to the deviation from the peaking approximation can be computed exactly if we assume that only one photon is emitted by using the standard perturbation theory.[5] All we have to do is to relate the momentum distribution of the photon to that of q' using the relation $q'=q-k$ and $d^3q'=d^3k$. If one photon emission is assumed, the probability distribution of the virtual photon becomes unnormalizable. However we know how to take care of this; all we have to do is to multiply the result by a factor $(v_s v_p)^{bt_r}$ as we did in Eq. (3.1).

The point of view expressed in this chapter can obviously be used in the $e^+ + e^-$ colliding beam experiments. In this case $\underset{\sim}{s} = -\underset{\sim}{p}$, hence $Q=0$ (see Fig. 6). An expanded version of the content of this chapter will be published elsewhere.

6. CONCLUDING REMARKS

Radiative corrections are indispensible in any electron scatterings because the raw data is hard to interpret theoretically. The procedures for the radiative corrections as presented in these lectures are the results of accumulated efforts by many people. The list of references given in this note did not do justice to many people who have contributed to this effort. More comprehensive lists of references can be found in the review articles by H. Uberall[31] and L. C. Maximon.[32] A short summary by D. B. Isabelle[33] on the present status of the art can be found in this proceedings. The author would like to thank Prof. B. Basco for inviting him to the institute. Conversations with W. Bertozzi, L. C. Biedenbarn, H. S. Caplan, S. Kowalski at the institute influenced greatly the writing of this note. Finally I would like to thank D. R. Yennie, B. Chertok, R. Early, E. Bloom and G. Miller at SLAC for discussions on this subject.

The preliminary consideration on the radiative corrections to the coincidence experiments as presented in Chapter 5 was greatly motivated by the experiments being carried out at Cornell by Berkelman et al., Mo and Selove et al., and the experiment being carried out at SLAC by Toner et al. The author wishes to thank these gentlemen for discussions.

APPENDIX A

BORN APPROXIMATIONS

In this appendix, we summarize the results of the Born approximations for the nonradiative and the radiative cross sections.

1. Nonradiative Cross Sections

In the single arm inelastic e nucleus scattering where only the outgoing electron is detected, the cross section can be written in terms of Drell and Walecka's[21] $W_1(q^2, M_f^2)$ and $W_2(q^2, M_f^2)$:

$$\frac{d\sigma}{d\Omega dE_p} = \left.\frac{d\sigma}{d\Omega}\right)_{Mott} \left[W_2(q^2, M_f^2) + 2\tan^2\frac{\theta}{2}\, W_1(q^2, M_f^2)\right] \tag{A.1}$$

where

$$\left.\frac{d\sigma}{d\Omega}\right)_{Mott} = \frac{Z^2\alpha^2 \cos^2\frac{\theta}{2}}{4E_s^2 \sin^4\frac{\theta}{2}} \quad .$$

$$q^2 = -4E_sE_p \sin^2\frac{\theta}{2} = \nu^2 - Q^2 ,$$

$M_f^2 = q^2 + 2M\nu + M^2$ is the missing mass squared, ν and $\underset{\sim}{Q}$ are components of $q = s - p = (\nu, \underset{\sim}{Q})$ in the lab system, W_1 and W_2 are two invariant functions of q^2 and M_f^2, and are related to the matrix elements by

$$W_{\mu\nu} \equiv M^{-2}(t_\mu - q_\mu (t\cdot q)/q^2)\,(t_\nu - q_\nu (t\cdot q)/q^2)\, W_2 - (g_{\mu\nu} - q_\mu q_\nu/q^2)\, W_1$$

$$\equiv \sum_f \langle t|j_\mu(0)|f\rangle \langle f|j_\nu(0)|t\rangle\, (2\pi)^3\, (eZ)^{-2}\, \delta^4(q+t-p_f) \tag{A.2}$$

where t is the four momentum of the target particle (not Madelstam's t). The summation over the final states is automatically confined to a specific missing mass state $M_f^2=(q+t)^2$ by the δ function. We have normalized the states $|t\rangle$ and $|f\rangle$ such that all the factors such as $(m/E)^{1/2}$ $(2\pi)^{-3/2}$ associated with a fermion and $(1/2E)^{1/2}$ $(2\pi)^{-3/2}$ associated with a boson have been taken out from the matrix elements and given to the phase space so that both the matrix elements and the phase space become covariant. In any Lorentz frame where $t_x=q_x=q_y=0$ and $q=(q_0, q_z\hat{e}_z)$, we have from Eq. (A.2)

$$W_1(q^2, M_f^2) = W_{xx} \tag{A.3}$$

and

$$W_2(q^2, M_f^2) = M^2(t_z - q_z(t\cdot q)/q^2)^{-2}\left[W_{zz} - (q_0^2/q^2)\,W_{xx}\right] . \tag{A.4}$$

In the laboratory system $t=(M,0)$, $q=(\nu, \underset{\sim}{Q})$ we have

$$W_2(q^2, M_f^2) = q^4/(Q^2\nu^2)\left[W_{zz}^{lab} - (\nu^2/q^2)\,W_{xx}\right] . \tag{A.5}$$

Instead of W_1 and W_2, the experimental results are sometimes parameterized in terms of L. Hand's[22] longitudinal and transversal cross sections, $\sigma_S(q^2 M_f^2)$ and $\sigma_T(q^2, M_f^2)$ respectively. They are related to W_1 and W_2 by

$$W_2 = \frac{k}{4\pi^2 \alpha Z^2}\left(\frac{-q^2}{-q^2+\nu^2}\right)(\sigma_T + \sigma_S) , \tag{A.6}$$

$$W_1 = \frac{k}{4\pi^2 \alpha Z^2}\,\sigma_T , \tag{A.7}$$

where

$$k = \nu + q^2/2M . \tag{A.8}$$

In terms of matrix elements $W_{\mu\nu}$, σ_T and σ_S can be written as

$$\sigma_T = \frac{4\pi^2 \alpha Z^2}{k} W_{xx} \tag{A.9}$$

$$\sigma_S = \frac{4\pi^2 \alpha Z^2}{k} \left(\frac{-q^2}{\nu^2}\right) W_{zz}^{lab} \tag{A.10}$$

σ_T and σ_S are defined such that in the limit $q^2 \to 0$, σ_T reduces to the total photonuclear cross section at energy k, and $\sigma_S \to 0$. The factor k comes from the flux density. Since the incident flux is an ill defined concept for space like photons there is no compelling reason to use Hand's definition. Personally I would rather use the standard covariant flux density

$$\left[(q\cdot t)^2 - q^2 M^2\right]^{1/2} M^{-1} = Q \tag{A.11}$$

instead of k, because when q is time like, the flux density is a well defined concept and is given by Q in the laboratory system.

In terms of matrix elements we have

$$\frac{d\sigma}{d\Omega dE_p} = \left.\frac{d\sigma}{d\Omega}\right)_{Mott} \left[\left(\frac{-q^2}{Q^2} + 2\tan^2\frac{\theta}{2}\right) W_{xx} + \frac{q^4}{Q^2 \nu^2} W_{zz}^{lab}\right] \tag{A.12}$$

The Weissacker William's formula can be derived readily from this formula. We note that W_{xx} and W_{zz} are not singular when $q^2 \to 0$. Hence as $q^2 \to 0$ we may drop W_{zz}^{lab} in Eq. (A.12) and obtain (we have used Q instead of k in Eq. (A.9))

$$\frac{d\sigma}{d\Omega dE_p} \xrightarrow[q^2 \to 0]{} \frac{\alpha}{8\pi^2 Q \sin^2\frac{\theta}{2}} \left(\frac{E_s^2 + E_p^2 + 2E_s E_p \sin^2\frac{\theta}{2}}{E_s^2}\right) \sigma_\gamma(k) \tag{A.13}$$

The energy of the real photon has to be $k = \nu + q^2/2M$ in order to excite the same missing mass state.

When the missing mass is discrete, we define form factors $W^j_{1,2}(q^2)$ by

$$W_{1,2}(q^2, M_f^2) = W^j_{1,2}(q^2)\ \delta(M_f^2 - M_j^2)\, 2M \ . \tag{A.14}$$

When the discrete state has a finite width the δ function is replaced by a covariant Breit Wigner's formula[23]

$$\delta(M_f^2 - M_j^2) \longrightarrow \Gamma M_j\ \pi^{-1} / \left[(M_f^2 - M_j^2)^2 + \Gamma^2 M_j^2\right] \tag{A.15}$$

where Γ is the width which is a function of M_f^2. For example the width of the 3.3 resonance can be written as

$$\Gamma(M_f^2) = 0.1293\ \text{GeV}\ \frac{0.85\,(p^*/m_\pi)^3}{1 + \left[0.85\,(p^4/m_\pi)\right]^2} \tag{A.16}$$

$$p^* = \left[(M_f^2 - M_p^2 + m_\pi^2)/(2M_f)\right]^2 - m_\pi^2 \ .$$

Substituting Eq. (A.14) into Eq. (A.1) and integrating the expression with respect to dE_p, we obtain the differential cross section for excitation of the jth level

$$\frac{d\sigma_j}{d\Omega} = \left.\frac{d\sigma}{d\Omega}\right)_{\text{Mott}} \frac{2M}{2M + 2E_s(1 - \cos\ \theta)} \left[W_2^j(q^2) + 2\tan^2\frac{\theta}{2}\ W_1^j(q^2)\right] \tag{A.17}$$

For the elastic scattering from a proton (j=0)

$$W_2^o(q^2) = (G_e^2 + \tau\ G_m^2)/(1+\tau) \ , \tag{A.18}$$

$$W_1^o(q^2) = \tau\ G_m^2 \tag{A.19}$$

$$\tau = -q^2/4M^2 \tag{A.20}$$

and

$$G_e \approx G_m/2.793 \approx \left[1 - (q^2/.71\ \text{GeV}^2)\right]^{-2} \tag{A.21}$$

Equation (A.2) is the starting point of many of the theoretical discussions. Since Eq. (A.2) is true only in the first order Born approximation, all data has to be reduced into this form by applying the radiative corrections, Coulomb distortion corrections and the dispersion corrections.

Equation (A.2) can also be written in a slightly different form:

$$W_{\mu\nu} = \int e^{iq\cdot x} \langle t|j_\mu(x)|j_\nu(0)\ t\rangle\ d^4x\ (2\pi)^{-1}\ (eZ)^{-2} \tag{A.22}$$

$$= \int e^{iq\cdot x} \langle t|\left[j_\mu(x), j_\nu(0)\right]|t\rangle\ d^4x\ (2\pi)^{-1}\ (eZ)^{-2} \tag{A.23}$$

Equation (A.22) shows that $W_{\mu\nu}$ is essentially a fourier transform of the ground state expectation value of the space time correlation function. After inserting a complete set of states between $j_\mu(x)$ and $j_\nu(0)$ we see that Eq. (A.23) has an extra term proportional to $\delta^4(q-t+p_f)$, but this δ function is zero anyway so Eq. (A.23) is equivalent to Eq. (A.22). The commutation properties of two currents are of fundamental interest to theoretical physicists. It is hoped that by investigating the behavior of such commutators one may be able to find out what are the fundamental constituents of the elementary particles and whether field theory is necessary to describe a hadron.

The Weissacher-William's limit of the inelastic electron cross section, Eq. (A.13) is useful in estimating the small momentum transfer inelastic electron scattering cross section when the total photon cross section, $\sigma_\gamma(k)$, is known. It is also useful in experimentally determining $\sigma_\gamma(k)$ by doing small angle inelastic electron scatterings.[24]

When the final state is discrete it is sometimes convenient to further decompose W_{zz} into Coulomb multipoles and W_{xx} into magnetic and electric multipoles. This has been worked out in great detail by Durand et al.[25,23]

2. Radiative Cross Sections

It has been pointed out by many people[26] that as long as one-photon exchange is assumed and the hadron final states are unobserved, one can write any cross section in terms of W_1 and W_2, or σ_S and σ_T. If we assume one-photon exchange the bremsstrahlung cross section can also be written in terms of W_1 and W_2. Assuming one-photon emission, the radiative tail from the jth level can be written as[5]

$$\frac{d^2\sigma_{j,r}}{d\Omega dp} = \frac{\alpha^3}{(2\pi)}\left(\frac{E_p}{E_s}\right)\int_{-1}^{1} \frac{2M\omega d(\cos\theta_k)}{q^4(u_0 - |\underset{\sim}{u}|\cos\theta_k)}$$

$$\Bigg(W_2^j(q^2)\left\{\frac{-am^2}{x^3}\left[2E_s(E_p+\omega)+\frac{q^2}{2}\right]-\frac{a'}{y^3}\left[2E_p(E_s-\omega)+\frac{q^2}{2}\right]\right.$$

$$-2+2\nu\left(x^{-1}-y^{-1}\right)\left\{m^2(s\cdot p-\omega^2)+(s\cdot p)\left[2E_sE_p-(s\cdot p)+\omega(E_s-E_p)\right]\right\}$$

$$+x^{-1}\left[2(E_sE_p+E_s\omega+E_p^2)+\frac{q^2}{2}-(s\cdot p)-m^2\right]$$

$$\left.-y^{-1}\left[2(E_sE_p-E_p\omega+E_s^2)+\frac{q^2}{2}-(s\cdot p)-m^2\right]\right\}$$

$$+W_1^j(q^2)\left[\left(\frac{a}{x^3}-\frac{a'}{y^3}\right)m^2(2m^2+q^2)+4\right.$$

$$\left.+4\nu\left(x^{-1}-y^{-1}\right)(s\cdot p)(s\cdot p-2m^2)+\left(x^{-1}-y^{-1}\right)(2s\cdot p+2m^2-q^2)\right]\Bigg) \qquad \text{(A.24)}$$

where ω is the photon energy in the lab system

$$\omega = \frac{1}{2}(u^2-M_j^2)/(u_0-|\underset{\sim}{u}|\cos\theta_k)$$

$$u = s+t-p = p_f+k$$

$$u_0 = E_s+M-E_p$$

$$|\underset{\sim}{u}| = \left(u_0^2-u^2\right)^{1/2}$$

$$u^2 = 2m^2 + M^2 - 2(s\cdot p) + 2M(E_s - E_p)$$

$$q^2 = 2m^2 - 2(s\cdot p) - 2\omega(E_s - E_p) + 2\omega|\underset{\sim}{u}| \cos\theta_k$$

$$a = \omega(E_p - |\underset{\sim}{p}| \cos\theta_p \cos\theta_k)$$

$$a' = \omega(E_s - |\underset{\sim}{s}| \cos\theta_s \cos\theta_k)$$

$$b = -\omega|\underset{\sim}{p}| \sin\theta_p \sin\theta_k$$

$$\nu = (a' - a)^{-1}$$

$$\cos\theta_p = \frac{|\underset{\sim}{s}| \cos\theta - |\underset{\sim}{p}|}{|\underset{\sim}{u}|}$$

$$\cos\theta_s = \frac{|\underset{\sim}{s}| - |\underset{\sim}{p}| \cos\theta}{|\underset{\sim}{u}|}$$

$$x = (a^2 - b^2)^{1/2}$$

$$y = (a'^2 - b^2)^{1/2}$$

We have used the coordinate system as shown in Fig. 7. There is an uncertainty of zero divided zero when a'=a in Eq. (A.24). This happens just because of the particular factorization used in the ϕ_k integration, and there is nothing wrong with it. It occurs at an angle (notice a misprint in MT)

$$\cos\theta_k = \frac{1}{\sin\theta}\left[(E_s/|\underset{\sim}{s}|) \sin\theta_p - (E_p/|\underset{\sim}{p}|) \sin\theta_s\right],$$

which corresponds to the position of the minimum between the s and p peaks.[2] In numerical integration, a small area near this point should be ignored. In Eq. (A.24) we have eliminated all the redundant notations in MT because b=b' and $\nu=\nu'$ in this reference. We have also used W_1 and W_2 instead of G and F which were used in my original paper.[5]

APPENDIX B

STRAGGLING OF AN ELECTRON IN MATTER

In the electron scattering we are interested in the collision of an electron with a nucleus at an angle much larger than m/E where E is the energy of the incident or outgoing electron. However the electron has to pass through a medium of finite thickness before and after this large angle scattering. When an electron passes through a target, it loses some energy by ionization and bremsstrahlung. Ignoring the binding energy of the atomic electrons, the probability of the electron losing energy ϵ (per gm/cm^2) can be obtained from the Møller cross section and can be written as

$$W_i(E, G) = \frac{2\pi N\alpha^2}{m} \frac{Z}{A} \frac{1}{\epsilon^2} \left[1 + \frac{\epsilon^2}{E(E-\epsilon)}\right]^2$$

$$\equiv \frac{a}{\epsilon^2} \left[1 + \frac{\epsilon^2}{E(E-\epsilon)}\right]^2 \qquad \text{(B.1)}$$

where $N=6\times10^{23}$ is the Avogadro's number, m is the mass of the electron, Z and A are the atomic number and the atomic weight of the target material. The square bracket in Eq. (B.1) is due to the spin of the electrons. When ϵ is small this factor reduces to one, resulting in the Rutherford cross section. The corresponding quantity due to the bremsstrahlung emission can be written as[27]

$$W_b(E, \epsilon) = \frac{4N\alpha^3}{m^2} \frac{Z(Z+\eta)}{A} \ln(183Z^{-1/3}) \frac{b}{\epsilon} \phi\left(\frac{\epsilon}{E}\right) \qquad \text{(B.2)}$$

$$= \frac{1}{x_0} \frac{b}{\epsilon} \phi\left(\frac{\epsilon}{E}\right) \qquad \text{(B.3)}$$

where η is due to the bremsstrahlung emission in the ee scattering and is given by

$$\eta = \ln (1440\ Z^{-2/3})/\ln (183\ Z^{-1/3}) , \qquad \text{(B.4)}$$

$$b = \frac{4}{3} \left\{1 + \frac{1}{9}\left[(Z+1)/(Z+\eta)\right] \left[\ln (183\ Z^{-1/3}\right]^{-1}\right\} , \qquad \text{(B.5)}$$

and $\phi(v)$ is the shape of the bremsstrahlung spectrum normalized such that $\phi(0)=1$. When $E \geq 100$ MeV and $v \leq 0.8$, the intermediate screening formula can be used. When v is small, the screening is always complete, we have then

$$\phi(v) \approx 1-v+\frac{3}{4}v^2 \quad . \tag{B.6}$$

x_0 is the unit radiation length[27] in gm/cm^2.

From Eqs. (B.1) and (B.2) we see that even though the bremsstrahlung emission is proportional to α^3 compared with α^2 for the ionization, the former will dominate over the latter when

$$\frac{2\alpha}{\pi}(Z+\eta)\,\ell n\,(183\,Z^{-1/3})\,\frac{\epsilon}{m} \gg 1 \quad . \tag{B.7}$$

This means that when the energy loss is large (small) compared with $\sim$ 20 MeV/(Z+1), the bremsstrahlung process becomes more (less) important than the ionization. In our application, we expect the ionization is more important in affecting the shapes of discrete peaks, whereas the bremsstrahlung is more important when we are considering the tails far away from them. We also note that the ionization has a much shorter tail than the bremsstrahlung ($1/\epsilon^2$ versus $1/\epsilon$). When ϵ is so small that it is comparable to the binding energy of the electrons, we have to take into account of the binding of the electrons and the screening. This will in general make W_i less divergent than $1/\epsilon^2$ when ϵ approaches the binding energy.

Let us denote the probability of finding an electron in the energy interval between E and E+dE at a depth t (in units of radiation length) by $I(E_0, E, t)\, dE$ where E_0 is the energy of the electron at t=0. $I(E_0, E, t)$ satisfies the diffusion equation:

$$\frac{\partial I(E_0, E, t)}{x_0\,\partial t} = \int_0^{E_0-E} d\epsilon\; I(E_0, E+\epsilon, t)\left[W_i(E+\epsilon, \epsilon) + W_b(E+\epsilon, \epsilon)\right]$$

$$- I(E_0, E, t)\int_0^{E} d\epsilon \left[W_i(E, \epsilon) + W_b(E, \epsilon)\right] , \tag{B.8}$$

With the boundary condition,

$$I(E_0, E, 0) = \delta(E_0 - E) \quad . \tag{B.9}$$

When $W_i=0$, we obtain the straggling function due to the bremsstrahlung alone, $I_b(E_0, E, t)$. When $W_b=0$, we obtain the straggling function due to the ionization alone, $I_i(E_0, E, t)$. Let us define $\Delta \equiv E_0 - E$ and the Laplace transform of $I(E_0, E_0-\Delta, t)$ with respect to Δ as

$$L(E_0, p, t) = \int_0^\infty e^{-p\Delta}\, I(E_0, E_0-\Delta, t)\, d\Delta \quad . \tag{B.10}$$

Multiplying Eq. (B.8) by $e^{-p\Delta}$ and integrating with respect to Δ from 0 to ∞, we obtain

$$\frac{\partial L(E_0, p, t)}{x_0\, \partial t} = L(E_0, p, t) \int_0^\infty \left[W_i(\epsilon) + W_b(\epsilon)\right] e^{-p\epsilon}\, d\epsilon$$
$$- \int_0^{E_0-\Delta} \left[W_i(\epsilon) + W_b(\epsilon)\right] d\epsilon \int_0^\infty e^{-p\Delta}\, I(E_0, E_0-\Delta, t)\, d\Delta \tag{B.11}$$

Landau[13] approximated $E_0-\Delta$ by ∞ in one of the upper limits of the second integration. We cannot do this because $W_b(\epsilon)$ is proportional to $1/\epsilon$ and the integration diverges if we let $E_0-\Delta \rightarrow \infty$.

Let us obtain the solution for $I(E_0, E, t)$ by a more intuitive method. When $\left(E_0-E\right)/E_0 \ll 1$, we expect

$$I(E_0, E, t) \approx \int_E^{E_0} I_i(E_0, E', t)\, I_b(E', E, t)\, dE'$$
$$\approx \int_E^{E_0} I_b(E_0, E', t)\, I_i(E', E, t)\, dE' \quad . \tag{B.12}$$

This must be so because both $I_i(E_0, E_0-\Delta, t)$ and $I_b(E_0, E_0-\Delta, t)$ are relatively insensitive to the variation of E_0 when $\Delta \ll E_0$. If we accept (B.12), then from the convolution theorem of Laplace transform[28] we obtain

$$L(E_0, p, t) = L_b(E_0, p, t)\; L_i(E_0, p, t) \tag{B.13}$$

where

$$L_b(E_0, p, t) = \int_0^\infty e^{-p\Delta}\; I_b(E_0, E_0-\Delta, t)\, d\Delta \tag{B.14}$$

$$L_i(E_0, p, t) = \int_0^\infty e^{-p\Delta}\; I_i(E_0, E_0-\Delta, t)\, d\Delta\;. \tag{B.15}$$

Let

$$I_b(E_0, E_0-\Delta, t) = \frac{1}{\Gamma(bt)}\; \frac{1}{E_0}\; \left(\frac{\Delta}{E_0}\right)^{bt-1}\;. \tag{B.16}$$

We obtain from Eqs. (B.14) and (B.16),

$$L_b(E_0, p, t) = \frac{1}{(pE_0)^{bt}}\;. \tag{B.17}$$

According to Landau,[13]

$$L_i(E_0, p, t) = e^{-atx_0 p(1-0.5772-\ell n(p\epsilon'))}\;, \tag{B.18}$$

where a is defined in Eq. (B.1),

$$a = \frac{2\pi N\alpha^2}{m}\,\frac{Z}{A}\,\mathrm{cm}^{-2} = 0.154\ \mathrm{MeV}\ \frac{Z}{A}\;, \tag{B.19}$$

$$\ell n\,\frac{\epsilon'}{m} = \ell n\,\frac{I^2}{2E_0^2} + 1\;, \tag{B.20}$$

and $I = 13.5$ eV Z.

Using the inverse Laplace transform, we obtain

$$I(E_0, E_0-\Delta, t) = \frac{1}{2\pi i}\int_{c-i\infty}^{c+i\infty} e^{\Delta p}\, L(E_0, p, t)\, dp$$

$$= \frac{1}{2\pi i}\int_{c-i\infty}^{c+i\infty} \frac{e^{\Delta p - atx_0 p(1-0.5772-\ell n\, p\, \epsilon')}}{(pE_0)^{bt}}\, dp \qquad (B.21)$$

Landau[13] also showed that the most probable energy loss due to the ionization alone is given by

$$\Delta_0 = atx_0\left[\ell n\, \frac{atx_0}{\epsilon'} + 1-0.5772\right] \qquad (B.22)$$

In terms of Δ_0, we have

$$I(E_0, E_0-\Delta, t) = \frac{(ax_0t)^{bt-1}}{2\pi i E_0^{bt}}\int_{c-i\infty}^{c+i\infty} e^{p\left(\frac{\Delta-\Delta_0}{ax_0t}\right) + (p-bt)\,\ell n\, p}\, dp \qquad (B.23)$$

When b=0, we obtain Landau's result for I_i. The integration ($\lambda \equiv (\Delta-\Delta_0)/\xi$, $\xi \equiv ax_0t$)

$$F(\lambda, t) = \frac{1}{2\pi i}\int_{c-i\infty}^{c+i\infty} e^{p\lambda+(p-bt)\,\ell n\, p}\, dp \qquad (B.24)$$

has been carried out by J. Bergstrom,[11] assuming a small bt, bt ≤ 0.1. His result[11] is: when $\lambda \leq 10$

$$F(\lambda, bt) = f(\lambda)\left\{1+bt(1+\lambda)\right\} + \frac{(bt)^2}{2}\left\{-1+(\lambda+1)^2 f(\lambda) + \psi(\lambda)\right\} ;$$

when $\lambda \geq 10$,

$$F(\lambda, bt) = \frac{\omega^{bt}}{(1+\omega)\,\Gamma(1+bt)}\left[bt + \frac{1}{\omega}\right] \qquad (B.26)$$

where

$$f(\lambda) = F(\lambda, 0) = I_i(E_0, E_0 - \Delta_0 - \xi\lambda, t) \tag{B.27}$$

and

$$\psi(\lambda) = \int_\lambda^\infty f(\lambda')\, d\lambda' \tag{B.28}$$

are two universal functions given by Landau[13] in graphic forms. ω is the solution of the equation

$$\lambda = \omega + \ln \omega - 0.4228 \quad . \tag{B.29}$$

A useful approximation for ω is given by Borsch-Supan[29]:

$$\omega = \lambda \left(1 - \frac{\ln \lambda - 0.4228}{1 + \lambda}\right) \quad . \tag{B.30}$$

Landau showed that when $\lambda \geq 10$,

$$f(\lambda) \sim \frac{1}{\omega(\omega+1)} \tag{B.31}$$

and

$$\psi(\lambda) \sim \frac{1}{\omega} \quad . \tag{B.32}$$

For the calculation near the elastic peak we need an expression for

$$\int_{E_0-\Delta_0-\Delta E}^{E_0} I(E_0, E', t)\, dE = 1 - \int_0^{E_0-\Delta_0-\Delta E} I(E_0, E, t)\, dE \tag{B.33}$$

This relation is true if $I(E_0, E, t)$ is normalized correctly. Equation (B.12) shows that I will be normalized correctly if I_i and I_b are normalized correctly. Landau's I_i is normalized correctly but our Eq. (B.16) for I_b is not. This shows that if we want to calculate the left-hand side of Eq. (B.33) by using Eq. (B.26) in the right-hand side we must replace 1 in Eq. (B.33) by $1/\Gamma(1+bt)$. Hence

$$\int_{E_0-\Delta_0-\Delta E}^{E_0} dE\, I(E_0, E, t) = \frac{1}{\Gamma(1+bt)} \left[1 - \int_{\omega_{min}}^{E_0/\xi} \frac{d\omega}{\omega} \left(\frac{\omega}{E_0}\right)^{bt} \left(bt + \frac{1}{\omega}\right)\right]$$

$$\frac{1}{\Gamma(1+bt)} \left(\frac{\xi\, \omega_{min}}{E_0}\right)^{bt} \left(1 - \frac{1}{(1-bt)\, \omega_{min}}\right) \quad , \tag{B.34}$$

where ω_{min} is the value of ω, when $\lambda=\Delta E/\xi$. Using Eq. (B.30), we have

$$\omega_{min} = \frac{\Delta E}{\xi}\left(1 - \frac{\ln\frac{\Delta E}{\xi} - 0.4228}{1+\frac{\Delta E}{\xi}}\right) . \qquad (B.35)$$

Since Eq. (B.34) is true only when $\frac{\Delta E}{\xi} \geq 10$, we may approximately let $\omega_{min} = \frac{\Delta E}{\xi}$. Thus

$$\int_{E_0-\Delta_0-\Delta E}^{E_0} I(E_0, E', t) \approx (1+0.5722\,bt)\left(\frac{\Delta E}{E_0}\right)^{bt}\left(1-\frac{\xi}{(1-bt)\,\Delta E}\right) \qquad (B.36)$$

In order to satisfy $\Delta E/\xi \geq 10$, we must choose ΔE such that

$$\Delta E \geq 1.54 \text{ MeV} \frac{Z}{A} x_0 t \quad . \qquad (B.37)$$

On the other hand ΔE must be chosen small enough so that the cross section does not vary appreciably between $E-\Delta_0$ and $E-\Delta_0-\Delta E$. Especially in nuclear physics ΔE has to be chosen so that it is smaller than the distance between two neighboring levels if we want to resolve them. In order to simplify our presentation, we shall assume that the target thickness t is always chosen small enough so that in inequality (B.37) is satisfied.

For the calculation of a radiative tail, we need an expression for $I(E_0, E, t)$ in the interval $E_0-\Delta_0-\Delta E < E < 0.9\, E_0$. The expression for $I(E_0, E', t)$ obtained in Eqs. (B.23) and (B.26) can be written as

$$I(E_0, E, t)\,dE = \frac{1}{\Gamma(1+bt)}\left(\frac{\xi\omega}{E_0}\right)^{bt}\left(bt+\frac{1}{\omega}\right)\frac{d\omega}{\omega} \qquad (B.38)$$

This equation is true only when

$$10\xi/E_0 \leq (E_0-E)/E_0 \ll 1 \quad ,$$

hence it cannot be used to calculate the tail far away from the peak. However we know that in the limit of zero thickness, $I(E_0, E, t)$ must be proportional to the sum of the bremsstrahlung and ionization cross sections, hence

$$I(E_0, E, t)dE = \frac{tx_0}{\Gamma(1+bt)} \left(\frac{E_0-\Delta_0-E}{E_0}\right)^{bt} \left[W_b(E_0-\Delta_0, E_0-\Delta_0-E) + W_i(E_0-\Delta_0, E_0-\Delta_0-E)\right] dE \tag{B.39}$$

Equations (B.36) and (B.39) are the two formulas we need for dealing with the straggling effects. The physical meaning of Eq. (B.39) is as follows: When an electron goes through a medium it always suffers multiple scatterings accompanied by emission of soft photons and energy loss Δ_0 due to the ionization which is proportional to the target thickness. When the energy loss is large compared with Δ_0, most of the energy is lost either due to emission of a single photon or a single e-e scattering, and only a small fraction of the energy loss is due to the multiple photon emission and the ionization of many atoms. The gross features of $I(E_0, E, t)$ is thus determined by the sum of the cross sections for a single bremsstrahlung emission and a single e-e collision. The small correction due to the ionization of many atoms can be represented by substituting E_0 by $E_0-\Delta_0$ everywhere in the formula and the correction due to multiple photon emission is given to the factor

$$\frac{1}{\Gamma(1+bt)} \left(\frac{E_0-\Delta_0-E}{E_0}\right)^{bt} \approx (1+0.5772\, bt) \left(\frac{E_0-\Delta_0-E}{E_0}\right)^{bt} , \tag{B.40}$$

which has an effect of depleting the high energy component and increasing the low energy component of the electron spectrum.

The correction factor (B.40) is not very important in many experiments when E is far away from E_0. However in experiments such as obtaining the total γ + nucleus cross section by extrapolating the small angle e+nucleus scattering cross section,[24] the radiative tail from the elastic peak is sometimes responsible for

80 or 90% of the counting rate, and an error of 3% in the calculation of the radiative tail can cause an error of 30% in the experimental result. As mentioned previously when the energy loss is large the ionization loss is completely negligible compared with the bremsstrahlung loss, hence the uncertainty in its treatment will not cause a grave error. Eyges[30] showed that if the shape of the bremsstrahlung spectrum were given by (see Eq. (B.3)

$$\phi(v) = (1-v)^{a}\left[\ell n\,(1-v)\right]^{-1} \tag{B.41}$$

then Eq. (B.8), with W_i=0, can be solved analytically and be obtained

$$I_b(E_0, E, t) = \frac{tx_0(1+a)^{bt}}{\Gamma(1+bt)} \left(\frac{E}{E_0}\right)^a \left(\ell n\,\frac{E_0}{E}\right)^{bt} W_b(E_0, E_0-E) \tag{B.42}$$

Now the actual shape of the bremsstrahlung spectrum does not look like (B.41), but looks more like Eq. (B.6), when $E_0 > 1$ GeV and $v < 0.8$. Dr. R. Early[19] of SLAC solved Eq. (B.8) numerically by a computer, with W_i=0 and W_b given by the completely screened from, Eq. (B.6). His numerical results show that in this case the form

$$I_b(E_0, E, t) = \frac{tx_0}{\Gamma(1+bt)} \left(\frac{E_0-E}{E_0}\right)^{bt} W_b(E_0, E_0-E) \tag{B.43}$$

is accurate to within 0.5% for t=0.1 and for a thinner target the error is proportionally smaller. In this paper we shall use Eq. (B.43); the important thing to remember is to use a correct expression for the bremsstrahlung shape $\phi(v)$.[27]

APPENDIX C

TRIANGLE, HALF PATH LENGTH AND ENERGY PEAKING APPROXIMATION

Due to the straggling the observed cross section $\sigma_{exp}(E_s, E_p)$ is related to $\sigma_r(E_s, E_p)$ by

$$\sigma_{exp}(E_s, E_p) = \int_0^T \frac{dt}{T} \int_{E_{s\,min}(E_p)}^{E_s} dE_s' \int_{E_p}^{E_{p\,max}(E_s')} dE_p' \; I(E_s, E_s', t)$$

$$\sigma_r(E_s', E_p') \; I(E_p', E_p, T-t) \quad , \qquad (C.1)$$

where $I(E_0, E, t)$ is defined in Appendix B, $E_{s\,min}(E_p)$ and $E_{p\,max}(E_s')$ are determined by the kinematic boundary of $\sigma_r(E_s', E_p')$. This boundary is determined by the kinematics of the elastic scattering ($u^2 = M_f^2 = M^2$), hence

$$E_{p\,max}(E_s') = \frac{E_s'}{1 + E_s M^{-1}(1-\cos\theta)} \quad , \qquad (C.2)$$

and

$$E_{s\,min}(E_p) = \frac{E_p}{1 - E_p M^{-1}(1-\cos\theta)} \quad . \qquad (C.3)$$

This boundary is shown by the curved line labeled M_f=M in Fig. 4. Equation (C.1) means that the observed cross section $\sigma_{exp}(E_s, E_p)$ at point c in Fig. 4 is related to the magnitude of the cross section $\sigma_r(E_s', E_p')$ in the entire area a'b'c shown in Fig. 4. This area is called a triangle even though one of its side is a curve instead of a straight line. The curve becomes a straight line if we ignore the recoil as can be seen from Eq. (C.2). By definition $\sigma_r(E_s, E_p)$ is equal to $\sigma_{exp}(E_s', E_p')$ in the limit $T \rightarrow 0$. We shall use the trick repeatedly used in this paper. Namely we use an approximate expression for $\sigma_r(E_s, E_p)$ in order to simplify Eq. (C.1) and then at the end put the correct expression for $\sigma_r(E_s, E_p)$ back into the resultant formula. If we use the peaking approximation for σ_r and approximate the shape of the internal bremsstrahlung by that of the external bremsstrahlung (i.e., the method of equivalent radiators), then Eq. (C.1) is equal to replacing $\sigma_r(E_s', E_p')$ by $\sigma(E_s', E_p')$ times the factor $F(-2s'\cdot p', 0)$ introduced in Eq. (2.3) and adding two external radiators, each of thickness t_r defined in Eq. (2.7), one before and one after the scattering. In order to simplify the presentation we shall replace σ_r by σ in Eq. (C.1) and do all the modifications mentioned above later. We shall also ignore the ionization temporarily and only after Eq. (C.1) is reduced into a simpler form we put this effect back.

We first consider the contribution to Eq. (C.1) from a discrete state $M_f^2 = M_j^2$. After this is done we can integrate the resultant with respect to M_f^2 and obtain the entire contribution. When M_f^2 is a discrete state $M_f^2 = M_j^2$, the cross section $\sigma(E_s', E_p')$ contains a δ function (see A.14 and A.17)

$$\sigma(E_s', E_p') = \frac{d\sigma_j(E_s')}{d\Omega} \frac{1}{2M + 2E_s'(1-\cos\theta)} \delta((s'+t-p')^2 - M_j^2) \ . \tag{C.4}$$

The δ function reduces the <u>surface integration</u> $dE_s' dE_p'$ in the area a'b'c into a <u>line integration</u> along a curve labeled a"b" in Fig. 4.1. The integrand of (C.1) is very peaked near a" and b". We shall use this very peaked character of the integrand to simplify the expression. Let us consider a simple mathematical example. The behavior of our integrand is very similar to the integrand of the following integration:

$$\int_0^1 x^{T_i - 1} (1-x)^{T_f - 1} dx = \frac{\Gamma(T_i)\Gamma(T_f)}{\Gamma(T_i + T_f)} \ . \tag{C.5}$$

The answer happens to be the well known Beta function. Suppose we do not know how to do this integration and want to perform this integration by the peaking approximation:

$$\int_0^1 x^{T_i-1}(1-x)^{T_f-1}\,dx \approx \int_0^1 (1-x)^{T_f-1}\,dx + \int_0^1 x^{T_i-1}\,dx = \frac{1}{T_f} + \frac{1}{T_i} . \qquad (C.6)$$

When T is small, we have

$$\Gamma(T) = \frac{\Gamma(1+T)}{T} \approx \frac{1}{T}\left(1 - 0.5772\,T + O(T^2)\right) \qquad (C.7)$$

Hence

$$\frac{\Gamma(T_i)\,\Gamma(T_f)}{\Gamma(T_i+T_f)} = \left(\frac{1}{T_f} + \frac{1}{T_i}\right)\left(1 + O(T^2_{i,f})\right) \qquad (C.8)$$

Thus the error of the peaking approximation is $O(T^2_{i,f})$ compared with unity. In our case $T_i+T_f=bT < 0.1$, hence the error involved is less than 1%. Let us call this approximation <u>the energy peaking approximation</u> in contrast to <u>the angle peaking approximation</u> used in the calculation for the internal bremsstrahlung[2] (see Appendix C of MT). Using the energy peaking approximation Eq. (C.1) can be written as

$$\sigma_b^j(E_s, E_p) \equiv \int_0^1 \frac{dt}{T} \int_{E_{s\,min}(E_s)}^{E_s} dE'_s \int_{E_p}^{E_{p\,max}(E')} dE'_p \Bigg[I_b(E_s, E'_s, t)\,\frac{d\sigma_j(E'_s)}{d\Omega}$$

$$\frac{1}{2M+2E'_s(1-\cos\theta)}\,\delta\!\left(M^2 - M_j^2 + 2M(E'_s - E'_p) - 2E'_sE'_p(1-\cos\theta)\right) I_b(E'_p, E_p, T-t)\Bigg] \qquad (C.9)$$

$$\approx \int_0^T \frac{dt}{T}\Bigg[\frac{d\sigma_j(E_s)}{d\Omega}\, I_b(E_p+\omega_p, E_p, T-t) \int_{E_s-\omega_s}^{E_s} dE'_s\; I_b(E_s, E'_s, t)$$

$$+ \frac{d\sigma_j(E_s-\omega_s)}{d\Omega}\;\frac{M + (E_s-\omega_s)(1-\cos\theta)}{M - E_p(1-\cos\theta)}\; I_b(E_s, E_s-\omega_s, t)$$

$$\times \int_{E_p}^{E_p+\omega_p} dE'_p\; I_b(E'_p, E_p, T-t)\Bigg] \qquad (C.10)$$

where (see Fig. 4)

$$\omega_s = \frac{1}{2}(u^2 - M_j^2)/\left[M - E_p(1-\cos\theta)\right] \tag{C.11}$$

and

$$\omega_p = \frac{1}{2}(u^2 - M_j^2)/\left[M + E_s(1-\cos\theta)\right] \tag{C.12}$$

Equation (C.10) can be reduced further, and we finally obtain

$$\sigma_b^j(E_s, E_p) \approx (1+0.5772\,bT)\left[\frac{d\sigma_j(E_s)}{d\Omega}\frac{bT}{2}\frac{1}{\omega_p}\phi\left(\frac{\omega_p}{E_p+\omega_p}\right)\right.$$
$$\left.+\frac{d\sigma_j(E_s-\omega_s)}{d\Omega}\frac{M+(E_s-\omega_s)(1-\cos\theta)}{M-E_p(1-\cos\theta)}\frac{bT}{2}\frac{1}{\omega_s}\phi\left(\frac{\omega_s}{E_s}\right)\right]\left(\frac{\omega_s}{E_s}\right)^{bT/2}\left(\frac{\omega_p}{E_p+\omega_p}\right)^{bT/2} \tag{C.13}$$

After including the effects due to the ionization, the internal bremsstrahlung and the virtual photons, Eq. (C.13) becomes Eq. (3.1) in the text to calculate the radiative tail from a discrete state.

Equation (C.13) shows that the integration with respect to t can be approximated by assuming that the scattering took place exactly at $t=T/2$. The error involved in this approximation is discussed below. The integration with respect to t for the term proportional to $d\sigma_j(E_s)/d\Omega$ is

$$\int_0^T \frac{dt}{T}\frac{1}{\Gamma(b(T-t))\,\Gamma(1+bt)}\left(\frac{\omega_p}{E_p+\omega_p}\right)^{b(T-t)-1}\left(\frac{\omega_s}{E_s}\right)^{bt} \tag{C.14}$$

The correction to the half path length approximation must be proportional to bT for small T, hence we put

$$1+xbT = \lim_{bT\to 0} (Eq.(14))\Bigg/\left[\frac{1}{\Gamma\left(\frac{1}{2}bT\right)\Gamma\left(1+\frac{b}{2}T\right)} v_p^{\frac{bT}{2}-1} v_s^{\frac{bT}{2}}\right]$$

$$= \lim_{bT\to 0} 2\int_0^1 dy(1-y)\, v_p^{(1/2-y)bT}\, v_s^{(y-1/2)bT} \quad . \qquad (C.15)$$

Therefore,

$$x = 2\left[\frac{d}{d(bT)}\int_{-\frac{1}{2}}^{\frac{1}{2}} dz(1/2-z)\left(\frac{v_s}{v_p}\right)^{zbT}\right]_{bT=0}$$

$$= -\frac{1}{6}\ln\left(\frac{\omega_s}{\omega_p}\,\frac{E_p+\omega_p}{E_s}\right) \qquad (C.16)$$

Similarly the term proportional to $d\sigma_j(E_s-\omega_s)/d\Omega$ is multiplied by a factor $(1-xbT)$. Hence two corrections tends to cancel each other. $|x|$ is a very small number in general (< 0.1), hence the half path length approximation is indeed a very good approximation when $bT < 0.1$.

In the radiative correction to the jth peak we need an expression

$$\int_{E_{p\,max}}^{E_{p\,max}} \sigma_b^j(E_s, E_p)\, dE_p = \int_0^{\Delta E} \sigma_b^j(E_s, E_{p\,max}-\omega_p)\, d\omega_p \qquad (C.17)$$

where $E_{p\,max}$ is by definition (see Fig. 4)

$$E_{p\,max} \equiv E_p+\omega_p \quad . \qquad (C.18)$$

Hence instead of integrating with respect to E_p, we may integrate with respect to ω_p

Let

$$R \equiv \frac{\omega_s}{\omega_p} = \frac{M+E_s(1-\cos\theta)}{M-E_p(1-\cos\theta)} \approx \frac{M+E_s(1-\cos\theta)}{M-E_{p\,max}(1-\cos\theta)} \qquad (C.19)$$

which is almost a constant, because $E_p \approx E_{p\,max}$. Substituting Eq. (C.13) into Eq. (C.17) with the help of Eqs. (C.18) and (C.19), we obtain

$$\int_{E_{p\,max}-\Delta E}^{E_{p\,max}} \sigma_b^j(E_s, E_p)\, dE_p = (1+0.5772\,bT)\left(\frac{R\Delta E}{E_s}\right)^{bT/2}\left(\frac{\Delta E}{E_{p\,max}}\right)^{bT/2}\frac{d\sigma_j(E_s)}{d\Omega} \tag{C.20}$$

After including the effects due to the ionization, the internal bremsstrahlung and the virtual photons, Eq. (C.20) becomes Eq. (2.3) in the text to calculate the radiative corrections to a discrete level.

Since we know how to handle the contribution from a discrete state to the integration in Eq. (C.1), the result can be generalized readily to the contribution from the entire triangle a'b'c in Fig. 4.1. All we have to do is to integrate Eq. (13) with respect to M_f^2 from M^2 to u^2 which is the value of M_f^2 corresponding to the point c in Fig. 4. However it is a good idea to subtract all the contributions from the radiative tails of the discrete levels first before we untangle the continuum states. If this is done, M_f^2 should be integrated from the threshold of the continuum, M_c^2, instead of M^2. In contrast to the Born approximation, our integration with respect to M_f^2 converges at the point c in Fig. 4. However it is convenient to separate the integration with respect to M_f^2 into two regions (see Fig. 4):

$$M_c^2 < M_f^2 < u^2 - \Delta u^2 \equiv M^2 + 2M(E_s - R\Delta - E_p - \Delta) - 2(E_s - R\Delta)(E_p + \Delta)(1-\cos\theta)$$

and

$$u^2 - \Delta u^2 < M_f^2 \le u^2 \equiv M^2 + 2M(E_s - E_p) - 2E_sE_p(1-\cos\theta) ,$$

where R is defined by Eq. (C.19).

We have shown that if the energy peaking approximation is used, then in order to calculate the radiative tail from the jth peak, only the information of the nonradiative cross sections at points a" and b" is required. Hence for the continuum state, we need only the information of the cross sections on the lines a to c and b to c in Fig. 4.

$$\text{On the line ac:} \quad M_f^2 = M^2 + 2M(E_s' - E_p) - 2E_s' E_p (1 - \cos\theta) \qquad (C.21)$$

$$\text{On the line bc:} \quad M_f^2 = M^2 + 2M(E_s - E_p') - 2E_s E_p' (1 - \cos\theta) \quad . \qquad (C.22)$$

Using these relations we obtain finally the folding formula for the continuum region

$$\sigma_b^c(E_s, E_p) = (1 + 0.5772\,bT) \left[\left(\frac{R\Delta}{E_s}\right)^{bT/2} \left(\frac{\Delta}{E_p}\right)^{bT/2} \sigma(E_s, E_p) \right.$$
$$+ \int_{E_p+\Delta}^{E_{p\,max}(E_s)} dE_p' \, \sigma(E_s, E_p') \left(\frac{E_p' - E_p}{E_p'}\right)^{bT/2} \left(\frac{(E_p' - E_p)R}{E_s}\right)^{bT/2} \frac{bT}{2(E_p' - E_p)} \phi\left(\frac{E_p' - E_p}{E_p'}\right)$$
$$\left. + \int_{E_{s\,min}(E_p)}^{E_s - R\Delta} dE_s' \, \sigma(E_s', E_p) \left(\frac{E_s - E_s'}{E_p R}\right)^{bT/2} \left(\frac{E_s - E_s'}{E_s}\right)^{bT/2} \frac{bT}{2(E_s - E_s')} \phi\left(\frac{E_s - E_s'}{E_s}\right) \right] \qquad (C.23)$$

where R is given by Eq. (C.19).

Substituting Eq. (C.4) into Eq. (C.23) we obtain Eq. (C.13), hence the former is indeed the generalization of the latter. After including the effects due to the ionization, the internal bremsstrahlung and the virtual photons, Eq. (C.23) becomes Eq. (4.1) to calculate the radiative corrections to the continuum.

Equations (A.15), (A.16) and (A.17) of MT[2] should be replaced by Eqs. (C.20), (C.13) and (C.23) respectively of this paper.

REFERENCES

1. F. Bloch and A. Nordsieck, Phys. Rev. 52, 54 (1937).
2. L. W. Mo and Y. S. Tsai, Rev. Mod. Phys. 41, 205 (1969), hereafter referred to as MT.
3. Y. S. Tsai, Phys. Rev. 122, 1898 (1961).
4. N. T. Meister and D. R. Yennie, Phys. Rev. 130, 1210 (1963).
5. Y. S. Tsai, in Proceedings of the International Conference on Nuclear Structure, (1963), (Stanford University Press, Stanford, California, 1964) p. 221.
6. T. A. Griffy, D. S. Onley, J. T. Reynolds, and L. C. Biedenharn, Phys. Rev. 128, 833 (1962).
7. D. R. Yennie, F. L. Boos, Jr., D. G. Ravenhall, Phys. Rev. 137, B882, (1965).
8. G. H. Rawitscher, Phys. Rev. 151, 846 (1966).
9. Lectures in this proceeding by D. Drechsel, E. Kujawski, and Molinari.
10. J. D. Bjorken, Ann. Phys. (New York) 24, 201 (1963).
11. J. Bergstrom, in MIT 1967 Summer Study (Laboratory for Nuclear Science, MIT) 1967, p. 251.
12. H. Nguyen-Ngoc and J. P. Perez-y-Jorba, Phys. Rev. 136, B1036 (1964).
13. L. Landau, J. Phys. (USSR) 8, 201 (1944).
14. G. Källen, Encyclopedia of Physics Vol. 5/1 (Spinger Verlay, Berlin, 1958); p. 169.
15. J. Schwinger, Phys. Rev. 76, 790 (1949).
16. K. Mitchell, Phil. Mag. 40, 351 (1949).
17. D. R. Yennie, S. Frautchi, and H. Suura, Ann. Phys. (N.Y.) 13, 379 (1961).
18. D. R. Yennie (private conversation).
19. R. Early (SLAC Internal Memo, 1970, unpublished).
20. C. DeCalan and G. Fuchs, Nuovo Cimento 38, 1594 (1965).

20a. Y. S. Tsai, Phys. Rev. 137, B730 (1965).

21. S. D. Drell and J. D. Walecka, Ann. Phys. 28, 18 (1964).

22. L. N. Hand, Phys. Rev. 129, 1834 (1963).

23. A. J. Duffner and Y. S. Tsai, Phys. Rev. 168, 1801 (1968).

24. E. D. Bloom et al., International Symposium on Electrons and Photons at Liverpool (1969); p. 297, p. 251.

25. L. Durand, III, P. C. DeCelles and R. B. Marr, Phys. Rev. 126, 1882 (1962).

26. R. Von Gehlen, Phys. Rev. 118, 1455 (1960); M. Gourdin, Nuovo Cimento 21, 1094 (1961).

27. H. A. Bethe and J. Ashkin, Experimental Nuclear Physics, E. Segre, ed., (John Wiley and Sons, Inc., New York, 1953).

28. P. M. Morse and H. Feshbach, Methods of Theoretical Physics, (McGraw-Hill, Co., New York).

29. W. Börsh-Supan, J. Res. Nat. Bur. Stand. 65B, 245 (1961).

30. L. Eyges, Phys. Rev. 76, 264 (1949).

31. H. Überall, Radiative Corrections to Electron Scattering From Complex Nuclei, NRL Report 7080 (1970).

32. L. C. Maximon, Rev. Mod. Phys., 41, 193 (1969).

33. D. B. Isabelle and J. Berthot, Lecture at this institute.

FIGURE CAPTIONS

1. Born approximation graph in the electron scattering.
2. A typical example of spectrum in ep scattering. Both the raw data and the radiatively corrected data are shown. Only part of the elastic radiative tail is shown. It should be noted that after the subtraction of the elastic tail, the cross section between the elastic peak and the pion threshold becomes zero as it should. This graph was taken from Ref. 2.
3. The definition of ΔE. Notice that $E_p^{max} \neq E_p^{peak}$ in the definition of ΔE, but when integrating the cross section in Eq. (2.2) the limits of integration are $E_{p\,min}$ and $E_{p\,max}$. ΔE should be chosen much larger than the width to the right of the peak.
4. Triangles: Kinematic region necessary for radiative corrections to inelastic electron scattering.
5. Equivalent radiator method.
6. Kinematics of a virtual photon.
7. The coordinate system used in the integration with respect to the solid angle of the photon.

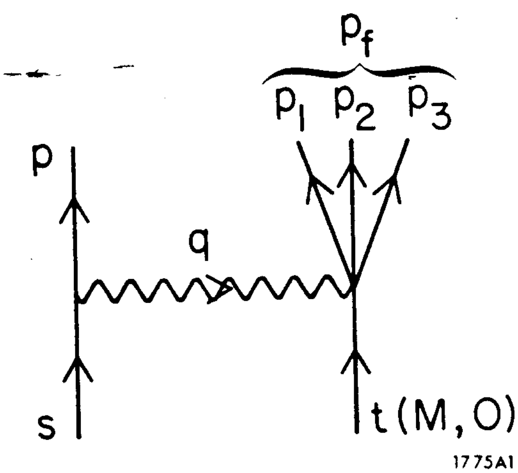

Fig. 1

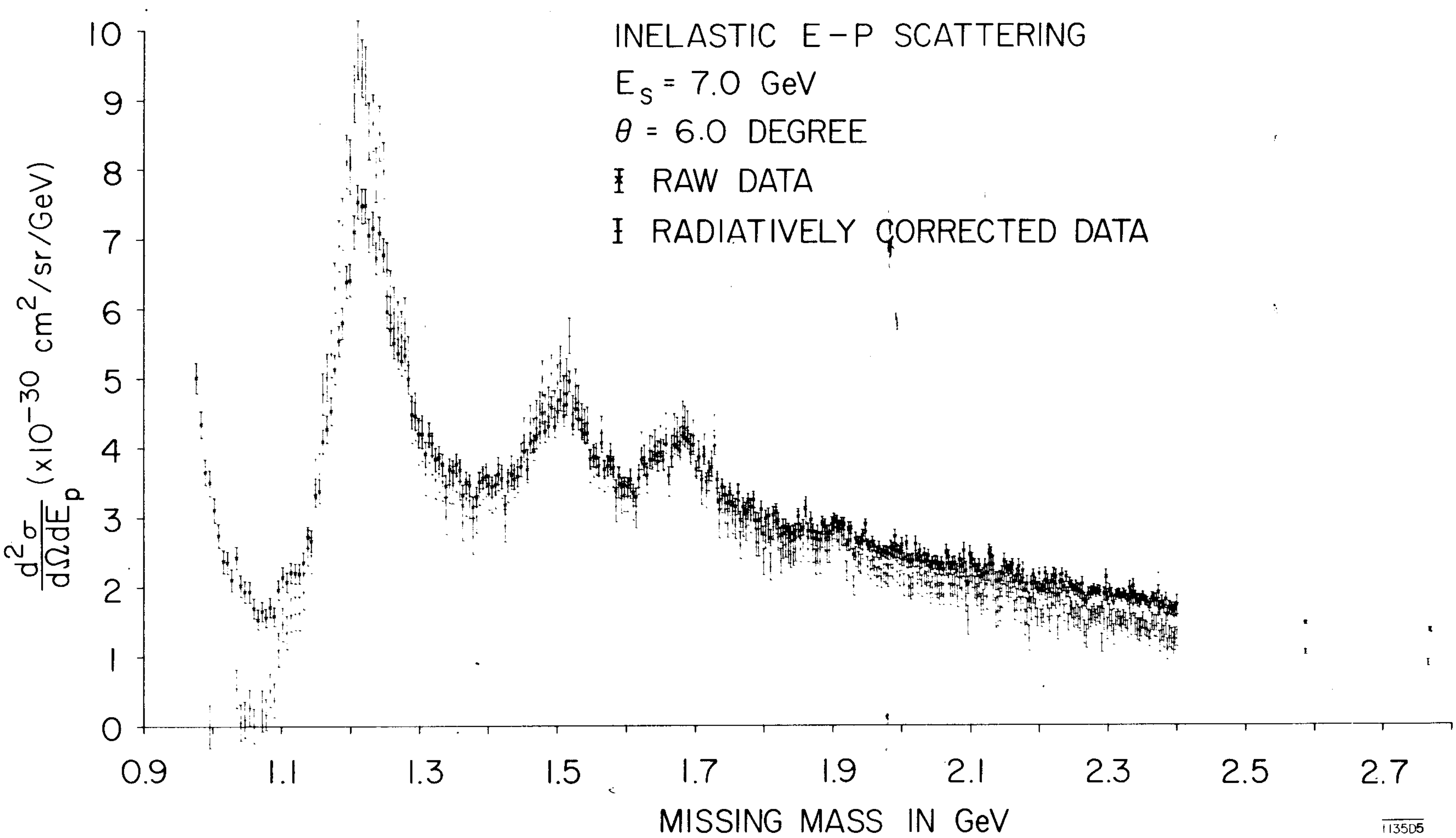
INELASTIC E-P SCATTERING
E_s = 7.0 GeV
θ = 6.0 DEGREE
RAW DATA
RADIATIVELY CORRECTED DATA
$\frac{d^2\sigma}{d\Omega dE_p}$ ($\times 10^{-30}$ cm^2/sr/GeV)
0
1
2
3
4
5
6
7
8
9
10
0.9
1.1
1.3
1.5
1.7
1.9
2.1
2.3
2.5
2.7
MISSING MASS IN GeV
1135D5

Fig. 2

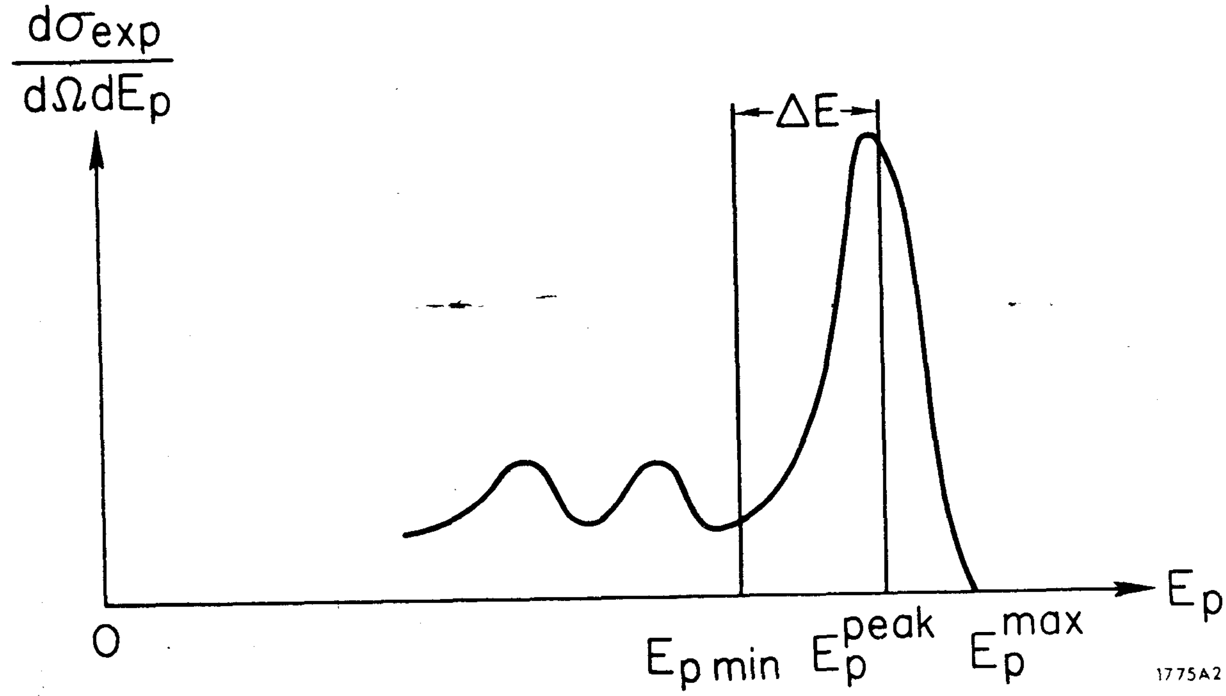

Fig. 3

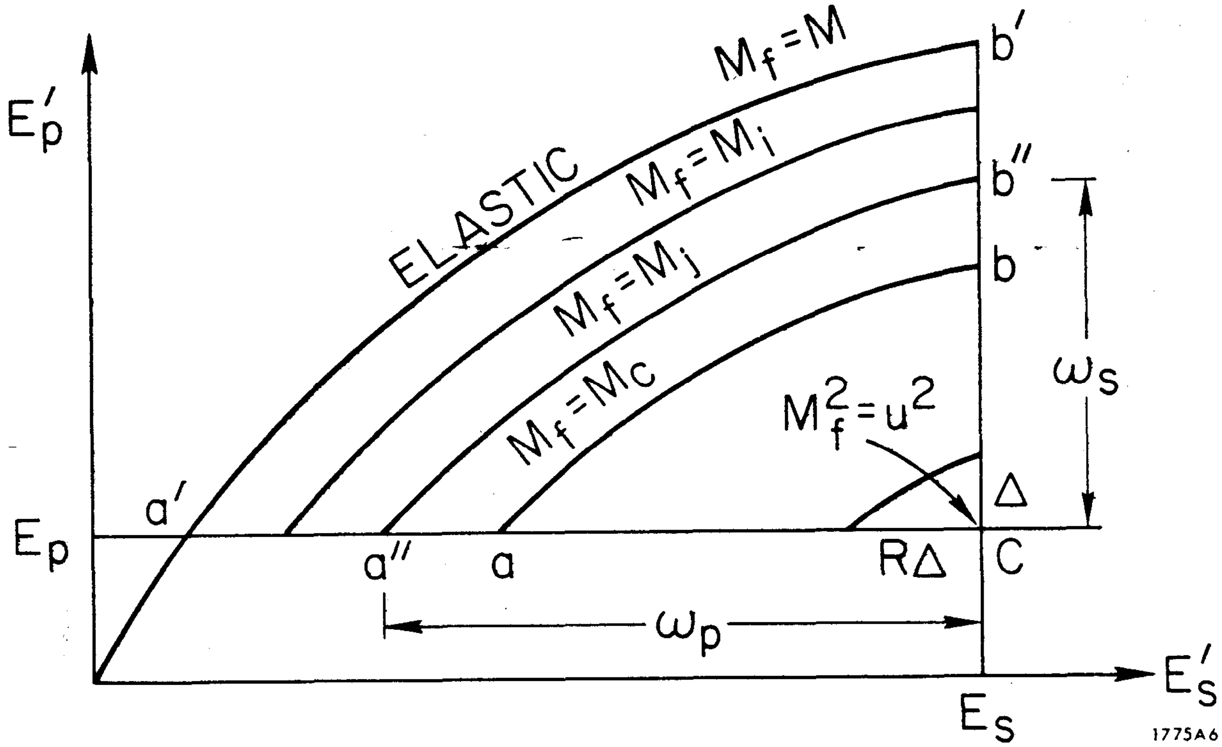
E_p'
ELASTIC
$M_f=M$
$M_f=M_i$
$M_f=M_j$
$M_f=M_C$
$M_f^2=u^2$
b′
b″
b
ω_s
Δ
a′
E_p
a″
a
RΔ
C
ω_p
E_s'
E_s
1775A6

Fig. 4

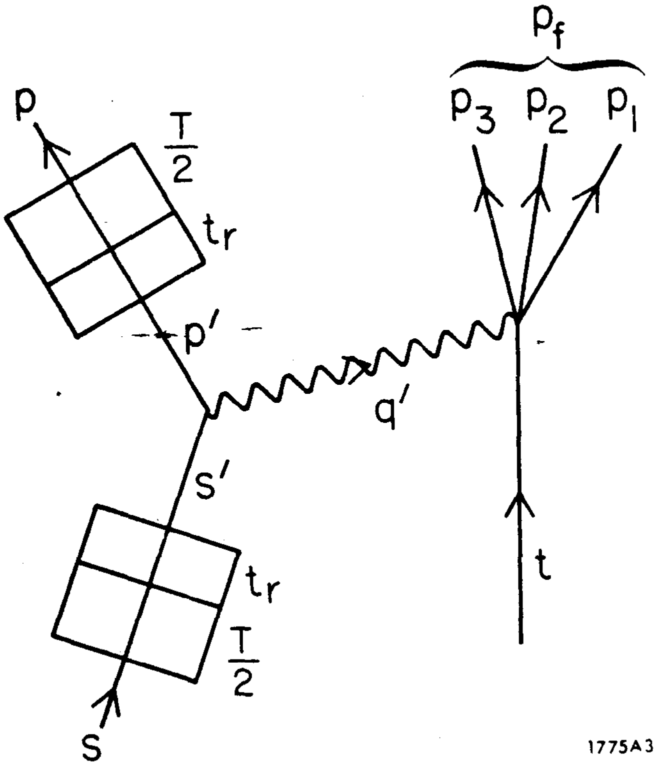

Fig. 5

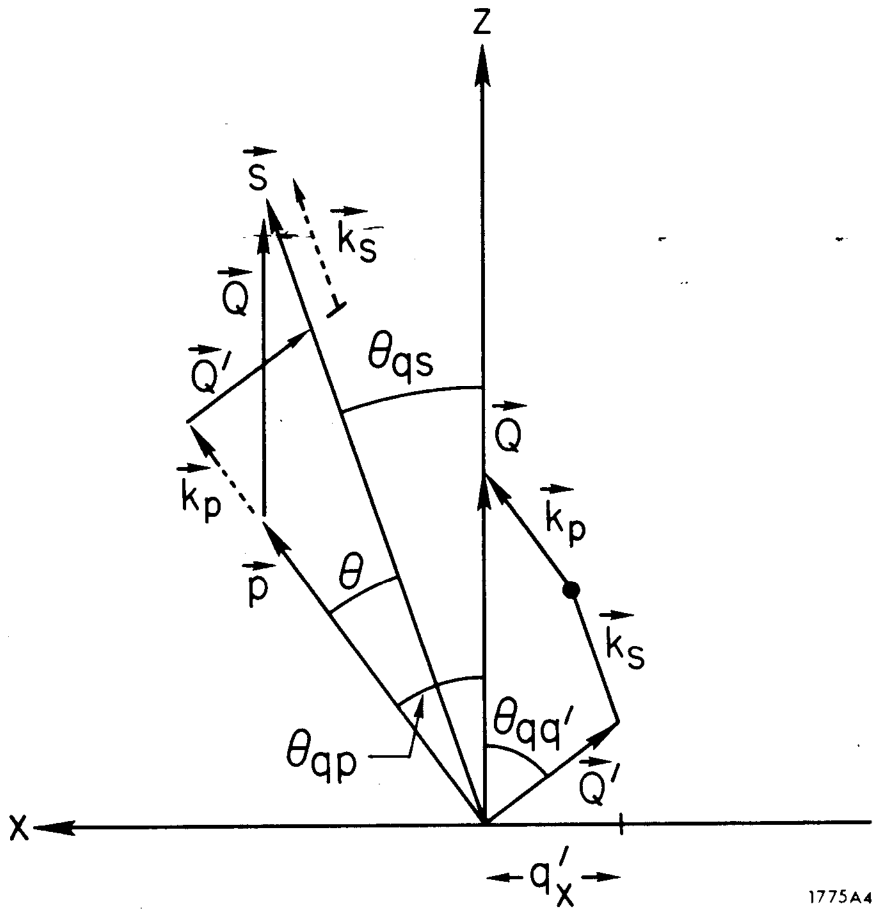
Z
X
$\vec{s}$
$\vec{k}_s$
$\vec{Q}$
$\vec{Q}'$
θ_{qs}
$\vec{Q}$
$\vec{k}_p$
$\vec{k}_p$
$\vec{p}$
θ
$\vec{k}_s$
$\theta_{qq'}$
θ_{qp}
$\vec{Q}'$
q_x'
1775A4

Fig. 6

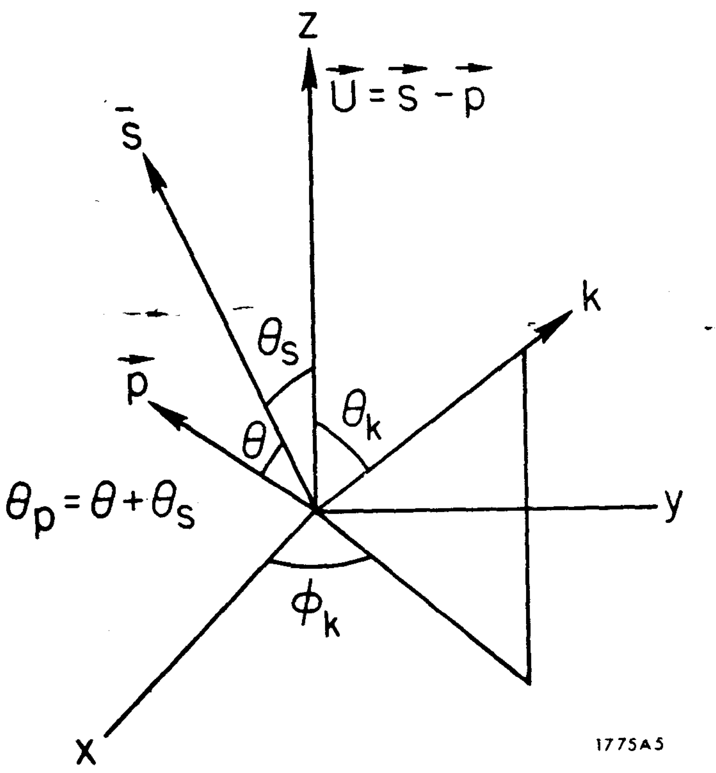

z
$\vec{U} = \vec{s} - \vec{p}$
$\bar{s}$
k
θ_s
$\vec{p}$
θ_k
θ
$\theta_p = \theta + \theta_s$
y
ϕ_k
x
1775A5

Fig. 7